INTERNATIONAL JOURNAL OF HEALTH & MEDICAL RESEARCH

ISSN(print): 2833-213X, ISSN(online): 2833-2148

Volume 05 Issue 07 July 2026

DOI : 10.58806/ijhmr.2026.v5i7n15

Page No. 672-694

Quantitative Isotope Tracer Methodologies for System-Level Metabolic Flux Analysis and Clinical Translation

Uba, Muhammad Tasi'u[1*], Ukairo, Doris Ifeyinwa[2], Nzebude, Chiamaka Perpetua[3], Ibrahim Mu'azu[4], Ukwueze, Thaddeus Onyebuchi[5], Okwaraejesu, Ugochukwu Valentine[6], Nwaekpe, Chinweuba Godswill[7,] Ismail, Yusuf Usman[8]

[1,2,3,5,6,7]Department of Biochemistry, School of Biological Sciences, Federal University of Technology, Owerri, Imo State, Nigeria.
[4,8]Department of Chemistry, School of Physical Sciences, Federal University of Technology, Owerri, Imo State, Nigeria.

ABSTRACT

Isotope tracer methodology provides a quantitative framework for investigating metabolic flux, substrate turnover and pathway compartmentalization in vivo. Tracer approaches enable dynamic examination of biochemical systems with minimal physiological perturbation, this can be achieved by harnessing the mass distinction and chemical equivalence of stable (e.g., ^{13}C, ^{15}N, ^{2}H) and radioactive (e.g., ^{14}C, ^{3}H, ^{18}F) isotopes. This review synthesizes the physicochemical basis of isotopic labeling, tracer dilution principles and nuclear decay mechanisms underlying scintillation detection and positron emission tomography (PET). Emphasis is placed on isotopologue distribution analysis using mass spectrometry (MS) (e.g. natural abundance correction, isotopic impurity adjustment, and resolution of spectral overlap: analytical considerations essential for accurate metabolic flux analysis). Applications in biomolecule (glucose, lipid, protein and glutamine) metabolism are examined, as well as ^{18}F-fluorodeoxyglucose PET and hybrid PET/computed tomography (translational imaging strategies). The safety, sensitivity, and spatial resolution levels of stable and radioactive tracers are comparatively evaluated. Critical methodological limitations (such as tracer recycling, steady-state assumptions, compartmental modeling limitations, and cost considerations) are addressed to define its limits in terms of interpretation. Emerging advances in multi-isotope tracing, high-resolution MS platforms, and integrated systems level modeling are discussed as future directions. When applied with rigorous quantitative discipline and transparent analytical correction, isotope tracer methodologies remain essential tools for revealing metabolic regulation, disease pathophysiology and therapeutic response.

KEYWORDS: Isotope tracers; ^{13}C metabolic flux analysis; stable isotopes; PET imaging; systems metabolism; pharmacokinetics; isotope-resolved metabolomics

INTRODUCTION

Isotope tracers represent a cornerstone technology in modern biomedical research and clinical medicine, enabling scientists and clinicians to visualize and quantify biological processes with unprecedented precision (Dimitrakopoulou-Strauss *et al*., 2024; European Society for Hybrid, Molecular and Translational Imaging [ESHMTI], 2024). The fundamental concept underlying isotope tracer methodology is elegantly simple yet profoundly powerful: by labeling specific molecules with isotopic variants of common elements, researchers can track the movement, transformation, and fate of these molecules through complex biological systems without significantly altering their inherent chemical behavior (Wolfe & Chinkes, 2017; Klein & Wolfe, 2022). This capability has revolutionized our understanding of human metabolism, disease pathophysiology, and therapeutic interventions across virtually every medical specialty, particularly in oncology, cardiology, neurology, and metabolic medicine (Ayeni *et al*., 2025; Hall & Guo, 2017).

The development of isotope tracer techniques dates back to the early 20th century, with pioneering work by George de Hevesy, who received the Nobel Prize in Chemistry in 1943 for his use of isotopes as tracers in chemical and biological processes (Nobel Prize Outreach, 2023). Since then, the field has evolved dramatically, driven by advances in analytical instrumentation, particularly mass spectrometry and nuclear imaging technologies, as well as improvements in isotope production and synthesis of labeled compounds (Calderoni *et al*., 2024; Kim *et al*., 2024). Today, isotope tracers serve dual roles in medicine: as research tools that elucidate the molecular basis of disease and as clinical diagnostic agents that guide patient management, especially through positron emission tomography (PET) and other hybrid imaging modalities (ESHMTI, 2024; Dimitrakopoulou-Strauss *et al*., 2024).

Quantitative Isotope Tracer Methodologies for System-Level Metabolic Flux Analysis and Clinical Translation

The clinical value of isotope tracers lies in their ability to provide functional and metabolic information that complements anatomical imaging such as CT and MRI (European Society for Hybrid, Molecular and Translational Imaging, 2024; Calderoni *et al*., 2024). By detecting molecular changes that often precede structural abnormalities, these techniques enable early diagnosis and improved assessment of treatment response and prognosis in diseases including cancer and endocrine disorders (Kim *et al*., 2024). In particular, ^{18}F-FDG PET has become essential in oncology for tumor detection, staging, and therapy monitoring, while emerging radiotracers further enhance personalized imaging approaches (Ayeni *et al*., 2025; Dimitrakopoulou-Strauss *et al*., 2024).

The application of isotope tracers extends beyond imaging to encompass detailed metabolic investigations using stable isotopes that pose no radiation risk (Bier, 1997; Wolfe, 1992). These stable isotope studies have illuminated the pathophysiology of diabetes mellitus, obesity, cardiovascular disease, and inherited metabolic disorders, leading to improved therapeutic strategies and personalized medicine approaches (American Diabetes Association, 2014; Hellerstein, 1999; Patterson *et al*., 2002). The ability to measure substrate oxidation rates, protein turnover, lipid metabolism, and energy expenditure in living humans has transformed metabolic research from descriptive observations to quantitative science (Hall, 2012; Wolfe, 1992).

This comprehensive review examines the principles underlying isotope tracer methodology, the different types of isotopes employed in biomedical applications, mechanisms of isotope detection and quantification, and practical applications in clinical medicine with particular emphasis on glucose metabolism as an exemplar system. The sophisticated instrumentation required for isotope measurement was explored, from mass spectrometers capable of detecting single atoms to imaging devices that visualize tracer distribution throughout the body. Understanding these concepts is essential for students and researchers seeking to apply isotope tracer techniques to address fundamental questions in human biology and medicine.

2. FUNDAMENTAL PRINCIPLES OF ISOTOPE TRACING

2.1 Atomic Structure and Isotopic Variation

Isotopes are atoms of the same chemical element that contain identical numbers of protons but differ in their neutron content, resulting in different atomic masses. This relationship is expressed mathematically as:

A = Z + N

Where A represents the mass number (total nucleons), Z denotes the atomic number (protons), and N indicates the number of neutrons. The existence of isotopes arises from the quantum mechanical properties of the atomic nucleus, where varying neutron numbers can produce stable or unstable nuclear configurations (Wolfe & Chinkes, 2005).

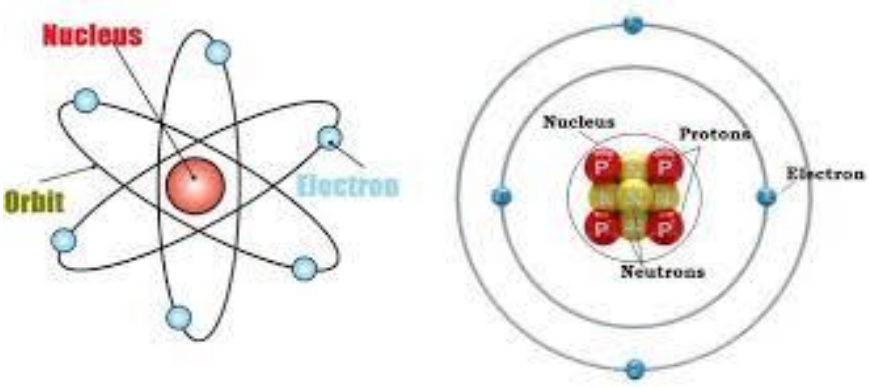

Figure 1.1. Atomic Structure and Isotopic Variation

Isotopes of a chemical element share the same atomic number (Z; number of protons) but differ in neutron number (N), resulting in different mass numbers (A = Z + N). Although isotopes differ in nuclear mass, their identical electronic configuration confers nearly identical chemical behavior. This chemical equivalence enables isotope tracer methodology, allowing labeled molecules to participate in biochemical reactions without significantly perturbing physiological systems.

Isotopic tracers are quite effective, because, although isotopes are distinct from each other in their physical characteristics, they have the same chemical behavior (they are chemically equivalent), as they have the same proton number and electronic configuration. Therefore, they can track metabolic processes without significantly disrupting the system. (Bier, 1987).

2.2 The Tracer Dilution Principle

A cornerstone concept in isotope tracer methodology is the dilution principle, which states that when a known quantity of labeled tracer is introduced into a system containing unlabeled material (tracee), the extent of dilution directly reflects the pool size of the tracee. This relationship is quantified by:

$$Q = \frac{qx\ Etrace}{Emix}$$

Figure 2.1. ***The Tracer Dilution Principle***

Where Q represents the unknown quantity of tracee, q is the known quantity of tracer added, E_tracer is the enrichment of the pure tracer, and E_mix is the enrichment measured after complete mixing. This principle underlies numerous clinical applications, from measuring blood volume and cardiac output to determining rates of glucose production and protein turnover (Wolfe & Chinkes, 2005).

Enrichment is typically expressed as atom percent excess (APE), which quantifies the percentage of atoms of a particular isotope above natural abundance levels. The calculation accounts for the isotope ratio before and after tracer administration, correcting for the small amounts of heavy isotopes that occur naturally in biological systems.

2.3 Steady-State and Non-Steady-State Kinetics

In metabolic tracer studies, because tracer enrichment is constant, substrate kinetics are simple to calculate under isotopic steady state conditions, and substrate flux can be directly derived from infusion rate and plateau enrichment. However, dynamic conditions (e.g., feeding or exercise) require non-steady-state analysis using differential equation–based modeling to account for the changing tracer and substrate pools over time. (Cobelli *et al*., 1987).

3. TYPES OF ISOTOPES USED AS TRACERS

3.1 Stable Isotopes

Stable isotopes are non-radioactive variants that do not undergo spontaneous nuclear decay. Their principal advantage lies in their complete safety profile, allowing unlimited exposure without radiation concerns. This makes stable isotopes particularly appropriate for studies in children, pregnant women, and investigations requiring repeated measurements over extended periods (Wolfe & Chinkes, 2005).

The most commonly employed stable isotopes in biomedical research include:

- **Deuterium (^2H or D)**: The heavy isotope of hydrogen, with natural abundance of approximately 0.015%. Deuterium labeling is particularly useful for measuring body water turnover, energy expenditure via doubly labeled water ($^2H_2{}^{18}O$), and substrate oxidation (IAEA, 2022).

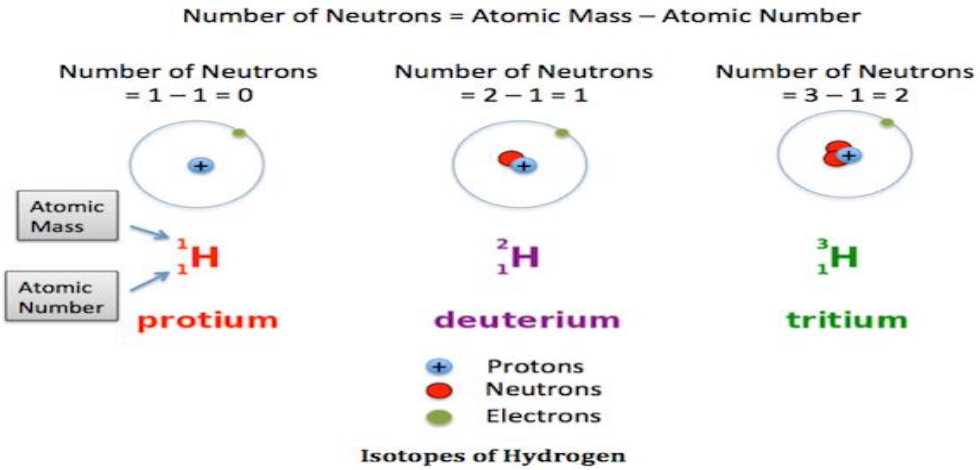

Figure 3.1.1. Isotopes of Hydrogen

Hydrogen isotopes include protium (^1H), deuterium (^2H), and tritium (^3H). Deuterium is applied in stable isotope tracing (e.g., ^2H_2O for body composition and lipid synthesis), whereas tritium is a beta-emitting tracer used in high-sensitivity radiolabeling studies.

- **Carbon-13 (^{13}C)**: Comprising approximately 1.1% of natural carbon, ^{13}C is extensively used for tracing metabolic pathways because carbon forms the backbone of all organic molecules. Position-specific ^{13}C labeling provides pathway-specific information about substrate metabolism (Jang *et al*., 2022; Klein & Wolfe, 2022).

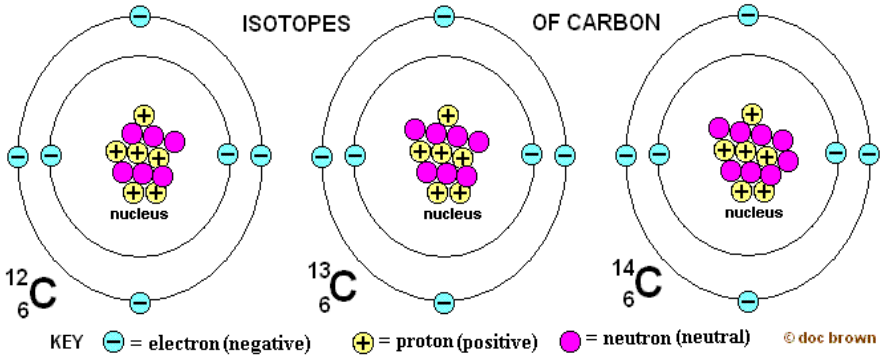

Figure 3.1.2. Isotopes of carbon

Carbon isotopes include stable ^{12}C and ^{13}C and radioactive ^{14}C. Carbon-13 is widely used in metabolic flux analysis due to nuclear stability and detectability by mass spectrometry (MS), whereas ^{14}C provides high radiometric sensitivity for kinetic and pharmacokinetic studies.

- **Nitrogen-15 (^{15}N)**: With natural abundance of about 0.37%, ^{15}N tracers are employed primarily for protein and amino acid metabolism studies, including measurements of protein synthesis, breakdown, and nitrogen balance (Klein & Wolfe, 2022; Wolfe *et al*., 2020).

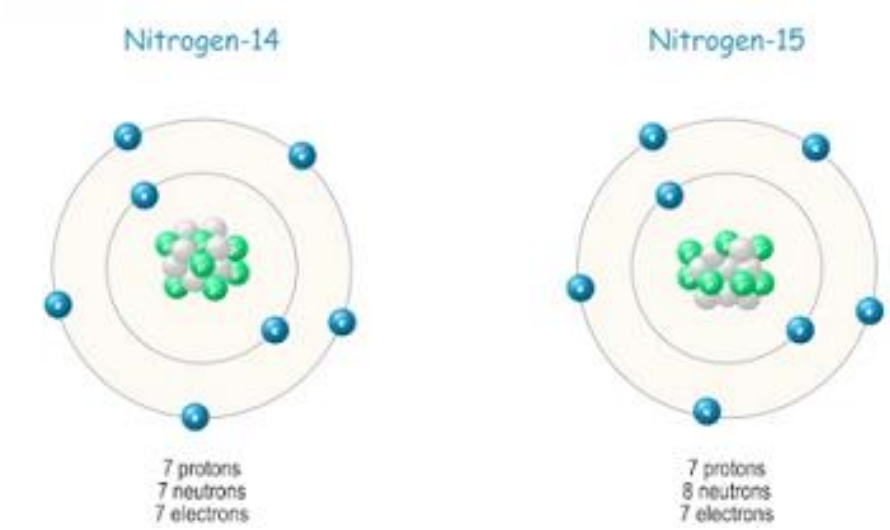

Figure 3.1.3. Isotopes of Nitrogen

Nitrogen occurs primarily as ^{14}N, with stable ^{15}N used in protein turnover and amino acid metabolism studies. Incorporation of ^{15}N into metabolic intermediates enables quantification of nitrogen flux and transamination pathways using MS-based isotopologue analysis.

- **Oxygen-18 (^{18}O)**: Comprising roughly 0.20% of natural oxygen, ^{18}O is used in doubly labeled water studies and for measuring metabolic water production and carbon dioxide production rates (IAEA, 2022).

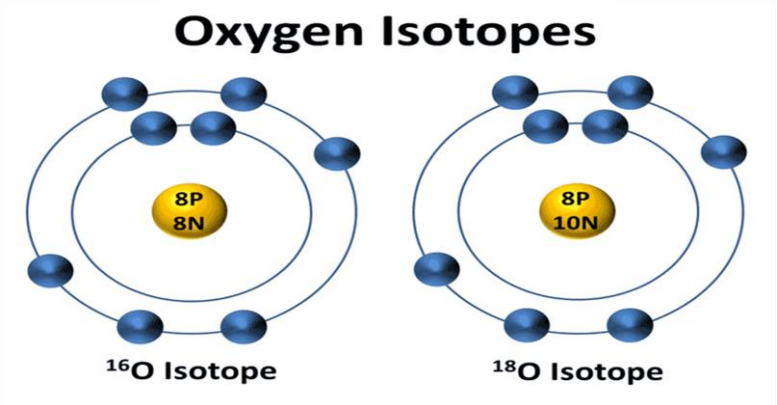

Figure 3.1.4. Stable Oxygen Isotopes Used in Metabolic Studies

Natural oxygen isotopes (^{16}O, ^{17}O, ^{18}O) and their relative abundances. Oxygen-18 (^{18}O; ~0.20% natural abundance) is widely used in doubly labeled water studies to quantify total energy expenditure and carbon dioxide production. Enrichment is measured by isotope ratio mass spectrometry (IRMS) with correction for natural abundance.

Sensitive detection of enrichment above baseline levels is made possible by the low natural abundance of stable isotopes. Researchers create isotopomers that offer comprehensive, pathway-specific metabolic information by labeling specific atomic positions, such as individual carbons in glucose or using uniformly labeled [U-$^{13}C_4$]glucose. (Kelleher & Masterson, 1992).

3.2 Radioactive Isotopes

IAEA, (2021); Cherry *et al*. (2021), radioactive isotopes (radioisotopes) undergo spontaneous nuclear decay, emitting radiation that can be detected with extraordinary sensitivity. The decay process follows first-order kinetics, with each radioisotope characterized by its half-life ($t_{1/2}$), the time required for half of the radioactive atoms to decay. The activity (A) of a radioactive sample, measured in becquerels (Bq) or curies (Ci), represents the rate of decay and decreases exponentially over time according to:

$A(t) = A_0\, e^{-\lambda t}$

where A_0 is the initial activity, λ is the decay constant, and t is time. The relationship between half-life and decay constant is:

$t_{1/2} = \frac{0.693}{\lambda}$

Clinically important radioisotopes are classified by their emission characteristics:

Beta-emitters release electrons (β^-) or positrons (β^+) during nuclear decay. Carbon-14 (^{14}C, half-life 5,730 years) emits low-energy beta particles and is extensively used in metabolic studies due to its long half-life and the ubiquity of carbon in biological molecules. Tritium (^3H, half-life 12.3 years) emits very low-energy beta particles that are easily shielded, making it safe for laboratory investigations (IAEA, 2021; Cherry *et al*., 2021).

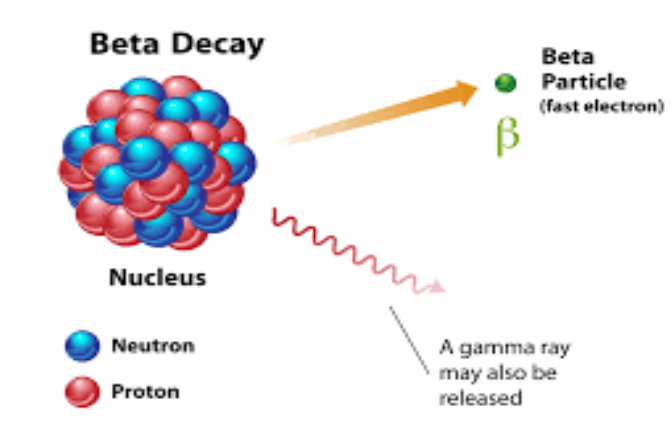

Figure 3.2.1: Beta (β^-) Decay Mechanism

Schematic of beta-minus decay in which a neutron converts into a proton with emission of an electron (β^-) and an antineutrino. Beta-emitting radionuclides such as carbon-14 (^{14}C) and tritium (^{3}H) are detected using liquid scintillation counting (LSC) and are widely applied in metabolic and pharmacokinetic studies due to high analytical sensitivity.

Positron-emitters are crucial for positron emission tomography (PET). Fluorine-18 (^{18}F, half-life 109.8 minutes) is the most clinically important PET isotope, incorporated into ^{18}F-FDG for metabolic imaging. Carbon-11 (^{11}C, half-life 20.4 minutes) enables labeling of molecules without altering their chemical structure, though its short half-life requires on-site cyclotron production (Phelps, 2000).

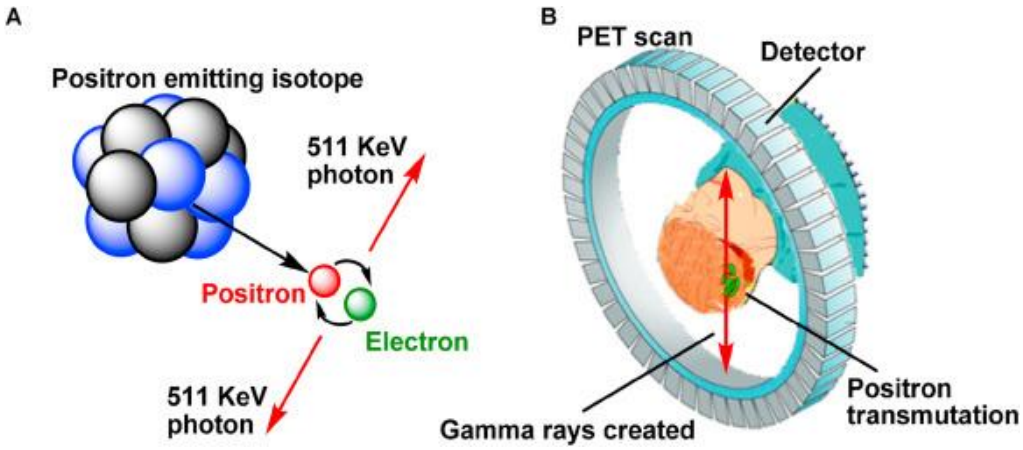

Figure 3.2.2: Positron Emission and Annihilation in PET Imaging

Positron (β^+) emission from radionuclides such as fluorine-18 (^{18}F). The emitted positron undergoes annihilation with an electron, producing two 511 keV gamma photons emitted at approximately 180°. Coincidence detection of these photons forms the physical basis of positron emission tomography (PET).

Gamma-emitters release high-energy photons and are used in single-photon emission computed tomography (SPECT). Technetium-99m (^{99m}Tc, half-life 6.01 hours, 140 keV gamma emission) accounts for approximately 80% of diagnostic nuclear medicine procedures. Iodine-123 (^{123}I, half-life 13.2 hours) and iodine-131 (^{131}I, half-life 8.02 days) are used for thyroid imaging and therapy (Schwochau, 1994).

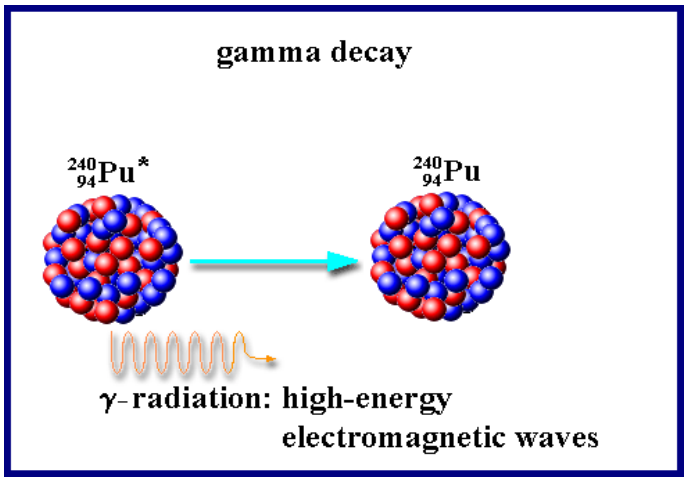

Figure 3.2.3: Gamma Photon Emission and Detection

Gamma emission from excited nuclear states (e.g., technetium-99m, ^{99m}Tc). Emitted photons are detected using gamma cameras or single-photon emission computed tomography (SPECT). Energy discrimination allows isotope-specific quantification.

Table 3.1 Quantitative Comparison: Stable vs Radioactive Tracers

Parameter	Stable Isotopes	Radioactive Isotopes
Examples	^{13}C, ^{15}N, ^{2}H, ^{18}O	^{14}C, ^{3}H, ^{11}C, ^{18}F

Detection	MS (ppm–ppb)	Scintillation, PET (femtomolar)
Sensitivity	~10^{-12} mol	~10^{-15} mol
Radiation Risk	None	Present
Regulatory Burden	Minimal	Strict
Imaging Capability	No (except hyperpolarized MRI)	Yes (PET/SPECT)
Cost per Study	High analytical cost	High isotope production cost
Clinical Repeatability	Unlimited	Dose-limited

4. MECHANISMS OF ISOTOPE DETECTION

4.1 Mass Spectrometry for Stable Isotopes

Mass spectrometry (MS), which ionizes molecules, separates ions according to their mass-to-charge ratio (m/z), and measures ion abundance with high sensitivity, is the standard method for detecting and quantifying stable isotopes, with the ability to detect enrichments below 0.01 percent above natural levels (Goodman & Brenna, 1992).

Isotope ratio mass spectrometry (IRMS) is the gold standard for accurate isotope ratio measurement in light elements. Such samples are converted to elemental gases (e.g., CO_2, N_2, and H_2 achieve precision better than 0.1 for ratios such as $^{13}C/^{12}C$ (Barrie & Prosser, 1996).

Gas chromatography-mass spectrometry (GC-MS) combines chromatographic separation with mass detection, often with selected ion monitoring (SIM) for high sensitivity, to allow compound-specific isotope analysis of complex mixtures (Patterson *et al*., 1993).

Liquid chromatography-mass spectrometry (LC-MS) expands tracer analysis to non-volatile and thermally labile compounds by reaching femtomole to attomole detection limits using tandem MS (MS/MS) and electrospray ionization (Chace, 2001).

4.2 Detection of Radioactive Isotopes

Liquid scintillation counting (LSC) is used to measure beta-emitting isotopes such as ^{3}H and $^{1°}C$ by mixing samples with a scintillation cocktail, which emits light pulses that are detected by photomultiplier tubes because of the beta particles. Multiple isotopes can be quantified simultaneously because pulse height is proportional to particle energy, with efficiencies of about 60–65 percent for ^{14}C and 40–50 percent for ^{3}H (L'Annunziata, 2012).

Gamma spectroscopy is used to measure gamma-emitting isotopes. Its characteristic energy peaks are used to identify and quantify the various isotopes (Knoll, 2010).

Positron emission tomography (PET) detects 511 keV photons produced by positron-electron annihilation. Clinical scanners today yield 3D images with 4-6 mm resolution from reconstructed events, while coincidence detection defines the line of response (Cherry *et al*., 2012).

5. GLUCOSE METABOLISM AND ISOTOPE TRACING

5.1 Glucose Structure and Labeling Strategies

Glucose ($C_6H_{12}O_6$) serves as the primary energy substrate for most mammalian cells and represents an ideal model system for understanding isotope tracer methodology in metabolism. The glucose molecule exists as a six-membered pyranose ring with carbons numbered C1 through C6. Each carbon position has distinct metabolic fates, making position-specific labeling particularly informative for pathway analysis (Basu *et al*., 2006).

Common glucose tracers include [1-^{13}C]glucose, [2-^{13}C]glucose, [6-^{13}C]glucose for position-specific labeling, [U-$^{13}C_6$]glucose for uniform labeling with stable isotopes, and [6,6-$^{2}H_2$]glucose for deuterium labeling. Radioactive tracers include [1-^{14}C]glucose, [6-^{14}C]glucose, and most importantly for clinical imaging, 2-[^{18}F]fluoro-2-deoxy-D-glucose (^{18}F-FDG). The choice of tracer depends on the specific metabolic question being addressed and the analytical methods available.

5.2 Glycolysis and the Tricarboxylic Acid Cycle

The ten steps of glycolysis are carried out in the cytoplasm and yield two ATP and two NADH from one molecule of glucose that is converted into two pyruvate. The process operates anaerobically and is regulated by three irreversible steps, hexokinase, phosphofructokinase-1, and pyruvate kinase, which respond to cellular energy status (ATP inhibits, AMP activates). The overall stoichiometry is:

Glucose + 2 NAD^+ + 2 ADP + 2 Pi → 2 Pyruvate + 2 NADH + 2 H^+ + 2 ATP + 2 H_2O

The TCA (Krebs) cycle oxidizes one acetyl-CoA molecule (derived from pyruvate) into CO_2 and produces three NADH, one $FADH_2$, and one GTP per cycle, generating about 30–32 ATP from oxidative phosphorylation fueled by these reducing equivalents. The cycle also provides biosynthetic precursors and is controlled by energy signals (ATP and NADH inhibit important enzymes) (Nelson & Cox, 2017).

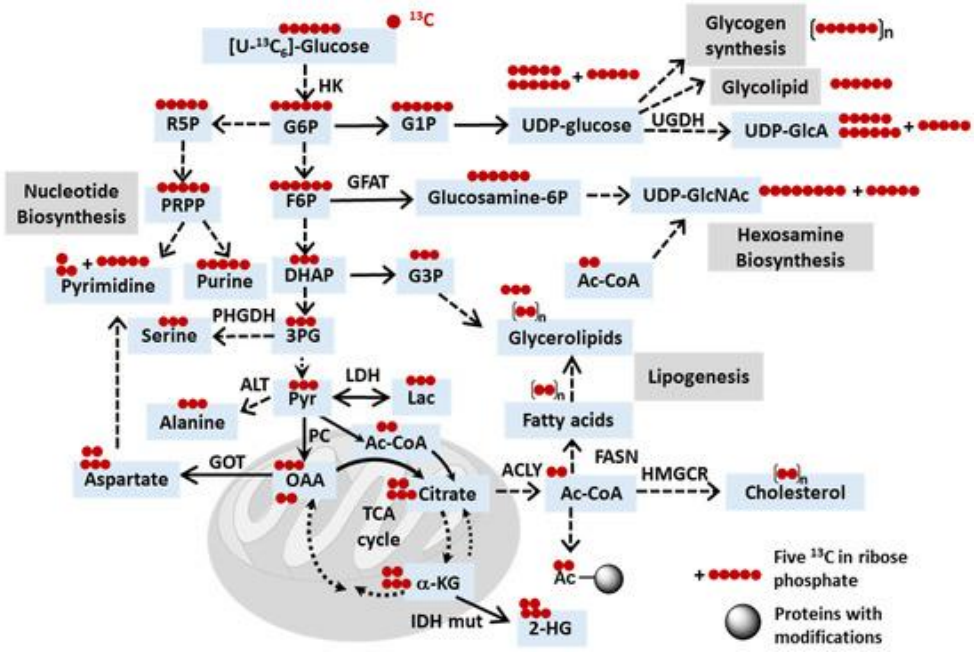

Figure 5.1: Isotopologue Distribution From [U-$^{13}C_6$]Glucose Metabolism

Schematic depicting the potential fates of ^{13}C in [U-$^{13}C_6$]glucose. Abbreviations: HK, hexose kinase; ACYL, ATP citrate lyase;IDH, isocitrate dehydrogenase; IDH mut, IDH mutant; UGDH, UDP-glucose dehydrogenase; GFAT, fructose-6-phosphate amidotransferase; PHGDH, phosphoglycerate dehydrogenase; LDH, lactate dehydrogenase; ALT, alanine transaminase; FASN, fatty acid synthase; GOT, glutamate-oxaloacetate transaminase 2; HMGCR, 3-hydroxy-3-methylglutaryl-CoA reductase; Ac, acetyl; G6P, glucose-6-phosphate; G1P, glucose-1-phosphate; F6P, fructose-6-phosphate; R5P, ribose-5-phosphate; PRPP, phosphoribosyl pyrophosphate; UDP-GlcA, UDP-glucuronate; UDP-GlcNAc, UDP-N-acetylglucosamine; DHAP, dihydroxyacetone phosphate; G3P, glycerol-3-phosphate; 3PG, 3-phosphoglycerate; Pyr, pyruvate; Lac, lactate; OAA, oxaloacetate; a-kG, alpha-ketoglutarate; 2-HG, 2-hydroxyglutarate.

When [U-$^{13}C_6$]glucose enters glycolysis, it produces [U-$^{13}C_3$]pyruvate, with the label distributed between both three-carbon products. The aldolase cleavage step splits the six-carbon intermediate into two three-carbon fragments, with C1-C3 of glucose forming one pyruvate and C4-C6 forming the other (Magnusson *et al*., 1992).

The tricarboxylic acid (TCA) cycle oxidizes acetyl-CoA derived from pyruvate decarboxylation, generating reducing equivalents for ATP synthesis. When [3-^{13}C]pyruvate (derived from [2-^{13}C]glucose) is decarboxylated by pyruvate dehydrogenase, it yields [2-^{13}C]acetyl-CoA, which condenses with oxaloacetate to form citrate. Due to the symmetric nature of succinate formed later in the cycle, carbon label becomes distributed among multiple positions in TCA cycle intermediates. Analysis of this isotopomer distribution by mass spectrometry reveals the relative activities of different metabolic pathways, including anaplerotic reactions that replenish cycle intermediates (Des Rosiers *et al*., 1994).

5.3 Measuring Glucose Production and Utilization

Endogenous glucose production (EGP) represents the sum of hepatic glucose release through glycogenolysis and gluconeogenesis. The glucose tracer dilution technique provides the gold standard method for EGP measurement. A constant infusion of labeled glucose, typically [6,6-$^2H_2$]glucose or [U-$^{13}C_6$]glucose, is administered until isotopic steady state is achieved, usually requiring 2-3 hours. At steady state, the EGP is calculated as:

$$EGP = \frac{Ftrace}{Eplasma} - Ftrace$$

where F_tracer is the infusion rate of the tracer and E is the plasma glucose enrichment at plateau (Steele, 1959). This approach has been instrumental in demonstrating that fasting hyperglycemia in type 2 diabetes results primarily from increased hepatic glucose production rather than decreased peripheral glucose utilization.

More sophisticated analyses distinguish gluconeogenesis from glycogenolysis by measuring the dilution of glucose tracers by unlabeled glucose arising from different sources. The incorporation of deuterium from body water (^2H_2O) into glucose carbon-bound hydrogens at specific positions provides information about gluconeogenic flux, since glycogenolysis releases preformed glucose without incorporating new hydrogen atoms (Landau *et al*., 1996).

5.4 PET Imaging with ^{18}F-FDG

In clinical medicine, the most commonly used PET radiotracer is F-FDG, which is used in millions of scans each year. The F-FDG is a glucose analog where the hydroxyl group at the C2 position is replaced with fluorine-18; it is transported into cells by GLUT transporters, phosphorylated by hexokinase, but it cannot enter glycolysis, and F-FDG-6-phosphate becomes trapped in proportion to the uptake of glucose (Gambhir, 2002).

The tracer emits positrons that are annihilated, producing paired 511 keV gamma photons that are detected, allowing for three-dimensional PET imaging. Tracer uptake is often quantified using the standardized uptake value (SUV), which normalizes tissue concentration to injected dose and body weight.

$$SUV = \frac{C\_tissue}{\frac{Injected\ Dose}{Body\ Weight}}$$

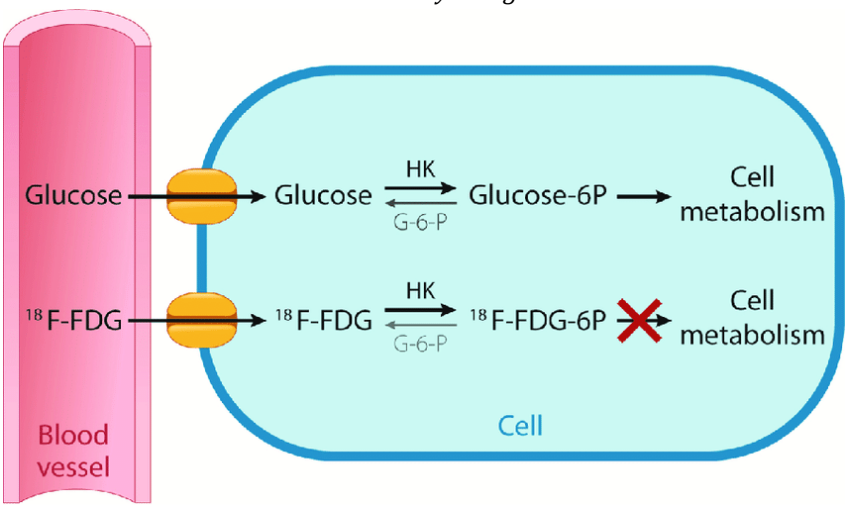

Figure 5.2: Cellular Uptake and Trapping of ^{18}F-Fluorodeoxyglucose (^{18}F-FDG)

Comparison of glucose and ^{18}F-FDG Cellular Uptake and Metabolism. Both enter the cells by glucose transporter membrane proteins. Once in the cell, both are phosphorylated by hexokinase (HK), which can be reversed by glucose-6-phosphatase (G-6-P) if present. Phosphorylated glucose (Glucose-6 P) is available to be further metabolized by the cell, whereas phosphorylated ^{18}F-FDG (^{18}F-FDG-6 P) cannot be further metabolized and is therefore considered "trapped".

Where C_tissue represents tissue tracer concentration. Higher SUV values indicate increased glucose metabolism, characterizing malignant tumors, inflammation, and regions of high metabolic activity in brain and heart (Huang, 2000).

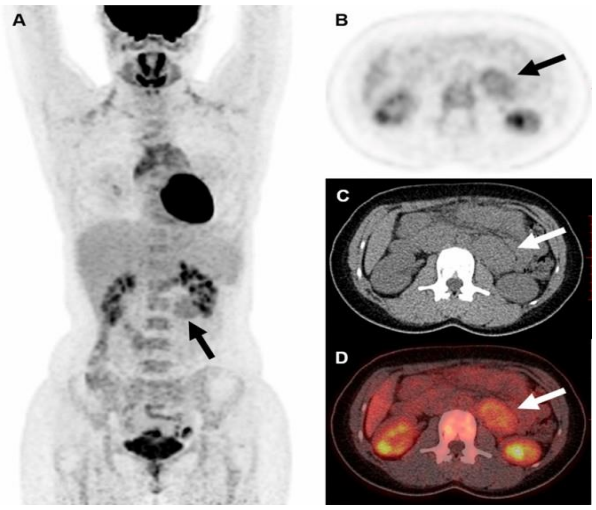

6.1 Isotope Tracers in Pharmacology: Drug Distribution, Metabolism, And Excretion

Drug disposition in the body is a complex process that involves multiple steps, including absorption, distribution, metabolism, and excretion (ADME). The ability to track the movement of drug molecules as they progress through tissues, are metabolized, and are

eliminated makes isotope tracer methodology an important tool in pharmacology, as it provides dynamic, real-time information on drug kinetics and pathways (Lappin & Temple, 2006).

The use of both stable isotopes (^{2}H, ^{13}C, ^{15}N) and radioisotopes (^{14}C, ^{3}H, ^{11}C, ^{18}F) provide complementary advantages, with the radioisotopes providing high sensitivity and enabling whole-body imaging, whereas stable isotopes are radiation-free and can be used for repeated studies. Incorporating variability into the metabolic profile has improved early pharmacokinetic assessment, reduced late-stage drug development failures, and supported personalized medicine (Penner *et al*. 2009).

Overall, isotope tracers offer a mechanistic basis for optimal drug therapy by being crucial for researching drug distribution, metabolism, excretion, interactions, and microdosing.

6.2 Principles of Isotope Labeling in Drug Studies

6.2.1 Isotope Selection and Labeling Strategies

The choice of isotope for labeling a pharmaceutical compound depends on multiple factors including the drug's chemical structure, the information sought, analytical capabilities, regulatory considerations, and safety requirements. Carbon-14 (^{14}C) remains the most widely used radioisotope in drug metabolism studies due to carbon's ubiquity in organic molecules and ^{14}C's long half-life (5,730 years), which eliminates concerns about radioactive decay during storage or extended studies. The beta particles emitted by ^{14}C have relatively low energy (maximum 156 keV), facilitating safe handling and waste disposal. Tritium (^{3}H) offers even lower energy emissions (maximum 18.6 keV) and can replace hydrogen atoms in virtually any organic molecule, though it may exchange with body water or be lost during metabolic reactions involving C-H bond cleavage, potentially complicating interpretation (Isin *et al*., 2012).

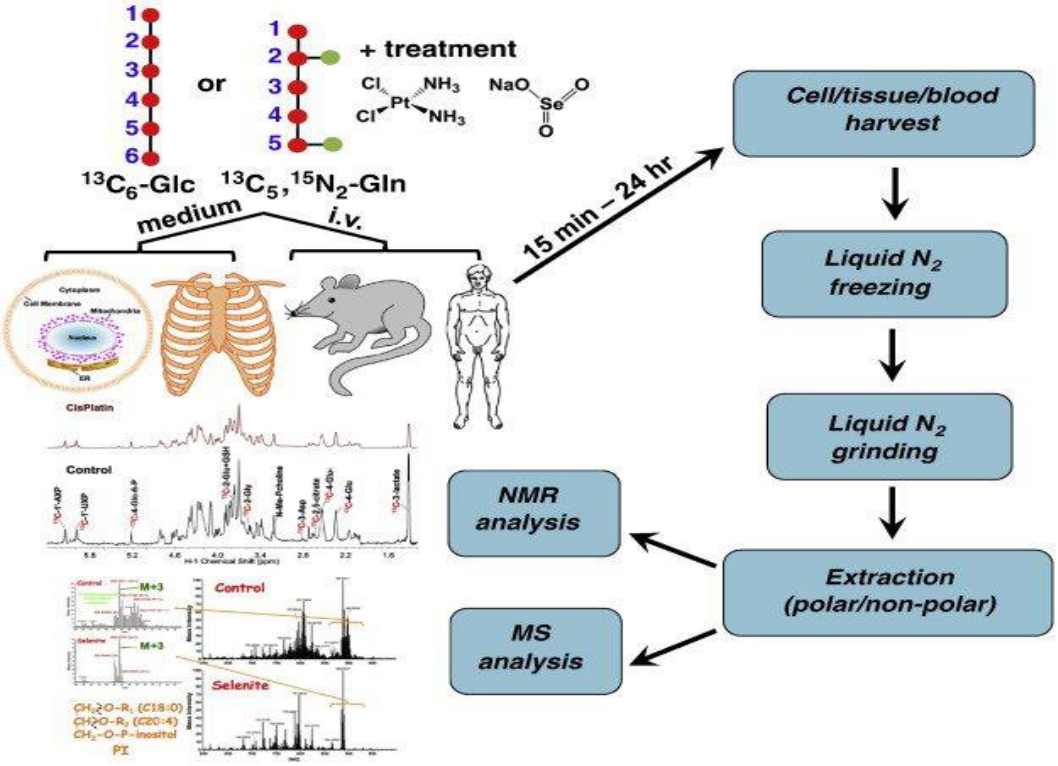

Figure 6.1: Isotope Labeling Strategies in Drug Metabolism Studies

Stable isotope labeling with ^{13}C, ^{15}N, and deuterium (^{2}H) is a non-radioactive, low-risk approach to use in human research, and although its heavier mass can result in kinetic isotope effects (KIEs), which typically slow reactions (2–7-fold for primary effects), deuterium is inexpensive and can be easily incorporated at multiple sites, as in the case of deutetrabenazine, where deuterium substitution lengthened the half-life and enhanced efficacy, although it altered drug metabolism (Timmins, 2014).

Position-specific labeling, where the isotope location is purposefully selected, allows identification of bond cleavage patterns, the differentiation of parent medications from metabolites, and the tracing of metabolic pathways; while uniform labeling, which limits the detail of the pathway, maximizes the detection signal. A good label ensures that the isotope remains attached to the target fragment during the analysis.

6.2.2 Specific Activity and Dosing Considerations

Specific activity (mCi/mmol or GBq/mmol) determines the amount of radioactive drug needed to produce a detectable signal while minimizing radiation exposure; higher specific activity allows for lower dosing. Because of the ability to incorporate multiple ^{3}H

atoms into a molecule, tritium can exceed 80 Ci/mmol, whereas ¹°C compounds are typically in the range of 10 to 60 mCi/mmol (Penner *et al*., 2009).

Regulatory guidance (ICRP, 2007) limits research exposure to ≤5 mSv per study and ≤10 mSv annually; typical ^{14}C studies (50–100 μCi) yield ~1–2 mSv. In contrast, stable isotope studies use doses of 1–10 mg to achieve detectable enrichment without radiation risk, thus allowing safe repeat and longitudinal studies.

6.3 Drug Distribution Studies

6.3.1 Absorption and Bioavailability

Absorption is the process by which a medication enters the bloodstream and, in the case of oral medications, involves hepatic portal passage, epithelial penetration, and gastrointestinal dissolution. Isotope-labeled compounds allow direct within-subject comparison, minimizing variability by administering IV and oral formulations with different labels to the same subject (Lappin *et al*. 2005), which can be used to quantify absolute bioavailability (F) by comparing oral and intravenous plasma exposure (AUC):

$$F = \frac{(AUCoral \times \text{DoseIV})}{(AUC\text{IV} \times \text{Dose}oral)}$$

Where AUC represents the area under the plasma concentration-time curve. Isotopologue discrimination is made possible by concurrent oral ($[^{13}C]$-labeled) and intravenous ($[^{11}C]$-labeled) dosing in the same subject, which reduces sample size and eliminates inter-occasion variability.

Because the labeled parent drug and metabolites can be monitored in portal and systemic circulation, isotope tracers can differentiate incomplete absorption from first-pass metabolism, quantify intestinal versus hepatic extraction, and inform formulation strategies such as prodrug design or permeability enhancement

6.3.2 Tissue Distribution and Volume of Distribution

Drug distribution is influenced by protein/tissue binding and physicochemical characteristics. Drug distribution can be described by the apparent volume of distribution ($V_d = \frac{\text{Dose}}{C_0}$) as a measure of the extent to which a drug leaves plasma; values greater than ~42 L (the total body water in an adult weighing 70 kg) indicate significant tissue uptake. Isotope-labeled medications provide accurate V_d determination through full mass balance tracking (Rowland & Tozer, 2011).

where C_0 is the plasma concentration immediately after intravenous administration. Large V_d values (exceeding total body water volume of approximately 42 L for a 70 kg person) indicate extensive tissue distribution, while small V_d values suggest restricted distribution primarily to plasma. Isotope-labeled drugs enable accurate V_d determination by providing definitive mass balance-all administered radioactivity or stable isotope-labeled drug can be accounted for in plasma, tissues, and excreta (Rowland & Tozer, 2011).

Whole-body autoradiography with ^{14}C or ^{3}H can visualize and quantify animal tissue distribution, which can show unexpected accumulation (e.g., G. melanin-rich tissues, bone), and guide toxicity assessment (Solon *et al*., 2010).

PET using positron emitters (^{11}C, ^{11}F, ^{11}O, and ^{13}N) noninvasively monitors drug kinetics, blood–brain barrier penetration, and receptor occupancy in humans; however, only 20–30% of some dopaminergic medications reach brain receptors (Piel *et al*., 2014).

6.3.3 Protein Binding and Free Drug Fraction

Only the unbound (free) fraction of a drug undergoes pharmacological effects, metabolism, and excretion; plasma protein binding affects distribution and elimination by lowering free concentration, primarily to albumin and α_2-acid glycoprotein. The free fraction (fu) is measured using equilibrium dialysis, ultrafiltration, or ultracentrifugation; for highly bound drugs (>99 percent), isotope-labeled drugs improve accuracy (Rowland & Tozer, 2011).

Isotope tracer studies also evaluate tissue binding, which can dramatically increase tissue concentrations and prolong elimination half-lives; in addition, displacement interactions between protein-bound medications are measured.

6.4 Drug Metabolism Studies

6.4.1 Metabolic Pathways and Metabolite Identification

The metabolism of medicinal products Lipophilic medicinal products are converted to hydrophilic metabolites through phase I functionalisation (oxygenation by cytochrome P450, reduction, hydrolysis) and phase II conjugation (e.g., glucuronidation, sulfation). Complete metabolite profiling is possible by radioisotope marking (e.g., |C), since all drug derived products keep the label and can be separated by HPLC and radioactivity detection (Hop *et al*., 1998).

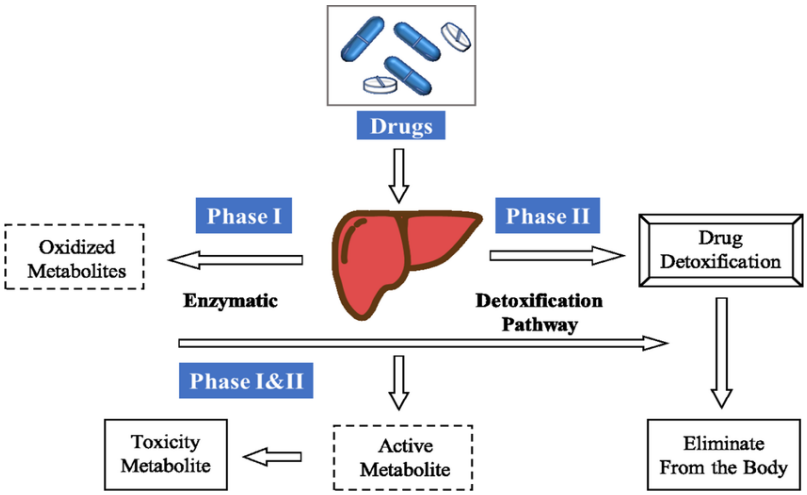

A different metabolite corresponds to each radioactive peak, and LC-MS identifies it by a mass difference that corresponds to the percent parent structure remaining. Tandem MS also detects structural changes, identifies toxic metabolites that cause hepatotoxicity (e.g., NAPQI acetaminophen), tracks stable isotope changes and isotopic patterns with high resolution MS, and identifies bioactive products (e.g., glutathione conjugates) and clarifies detoxification pathways (Koen & Hanzlik, 2002).

6.4.2 Cytochrome P450 Phenotyping and Reaction Phenotyping

CYP3A4, CYP2D6, CYP2C9, CYP2C19, and CYP1A2 are responsible for 80% of marketed drug metabolism in humans; reaction phenotyping to predict pharmacogenetic variability and drug–drug interactions based on which CYP isoforms metabolize a novel drug (Ogilvie *et al*. 2008).

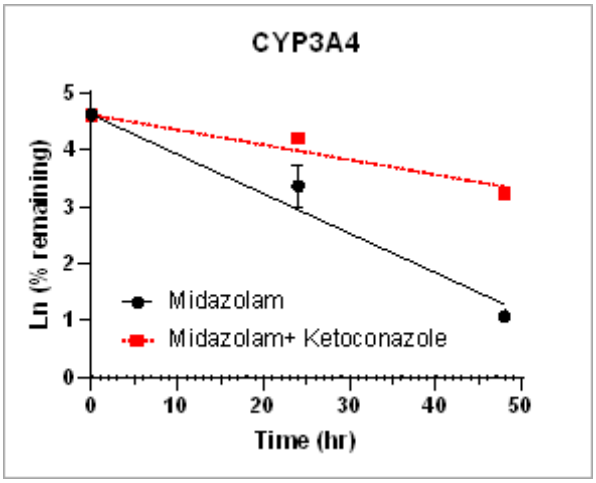

To quantify metabolites, isotope-labeled drugs are incubated with recombinant CYP enzymes or human liver microsomes, and enzyme involvement is confirmed using recombinant CYP systems, correlation analysis across liver microsomal panels, and selective chemical inhibitors (Ogilvie *et al*. 2008). Many antidepressants and antipsychotics are metabolized by CYP2D6, and genetically defined poor metabolizers have different reactions, indicating that they are a substrate for CYP2D6 (Zanger & Schwab, 2013).

Reactive metabolites can also irreversibly inactivate CYP enzymes, a form of inhibition called mechanism-based (suicide) inhibition (Khojasteh *et al*., 2011).

6.4.3 Metabolic Stability and Intrinsic Clearance

Isotope labeling allows assessment of metabolic stability as CLint using isotope-labeled drugs in microsomes or hepatocytes, substrate depletion kinetics predict in vivo hepatic clearance using physiologically based models (Obach, 1999). Isotope labeling increases analytical specificity, enhances mass balance, and facilitates optimization of high metabolic clearance compounds.

6.4.4 Metabolite Kinetics and Active Metabolites

Many drugs are metabolized to pharmacologically active metabolites that contribute to toxicity or efficacy, such as morphine-6-glucuronide, which has higher affinity than morphine at μ-opioid receptors. Isotope tracer techniques allow characterization of kinetics by separating metabolites made in vivo from those administered directly. Two kinetic models are applicable: In the formation-rate-limited model, the metabolite half-life is comparable to that of the parent drug because metabolite formation is slower

than elimination, while in the elimination-rate-limited model, the metabolite half-life is longer than the parent because formation is rapid, but elimination is slow, leading to accumulation with repeated dosing.

The rate-limiting step is determined experimentally by administering the labeled parent drug and labeled metabolite (with different isotopes) independently and comparing their terminal half-lives. For prodrugs, where the active metabolite controls dosage, this strategy is essential. Clopidogrel's active thiol metabolite, for example, is formation-rate-limited, according to [^{14}C] studies, which explains why loading doses are necessary to produce quick antiplatelet effects (Rehmel *et al*., 2006).

6.5 Drug Excretion Studies

6.5.1 Renal Excretion

Drugs are eliminated by the kidneys through passive reabsorption, active tubular secretion, and glomerular filtration. In mass balance studies, isotope-labeled medications are used to measure the percentage of a dose excreted in urine through full urine collection (48–168 hours).

Renal clearance ($CL\_R = \frac{\text{Amount Excreted}}{AUC}$) represents the plasma volume cleared per unit time. Cumulative urinary recovery (≥30–50 percent) indicates a significant renal contribution to clearance and the need for dose adjustment in renal impairment (Rowland & Tozer, 2011).

The mechanism is identified by comparing CLR with GFR (~120 mL/min) and the unbound fraction: ≈ fu·GFR indicates filtration; higher values indicate active secretion; lower values imply reabsorption. Proximal tubular OATs and OCTs are involved in secretion; transporter competition (e.g. G. Dosage adjustment may be necessary due to probenecid's inhibition of penicillin secretion (Giacomini *et al*., 2010).

6.5.2 Biliary Excretion and Enterohepatic Circulation

ATP-dependent ABC transporters (e.g., G. MRPs, BCRP, P-glycoprotein) are used by hepatocytes to excrete medications and metabolites into bile. In the enterohepatic circulation of biliary compounds, intestinal reabsorption also delays elimination and complicates pharmacokinetics. Biliary excretion and biliary clearance can be measured using isotope tracer studies with bile duct cannulation by measuring bile flow and drug concentration (Roberts *et al*., 2002).

Enterohepatic cycling, which results in secondary plasma peaks and prolonged terminal half-life, requires advanced modeling. Hydrolysis of glucuronide conjugates by colonic β-glucuronidases can regenerate the parent drug for reabsorption, as has been shown using ^{14}C labeling for mycophenolic acid and diclofenac. This cycle can be broken using binding resins or non-absorbable antibiotics to enhance drug removal (Shipkova *et al*., 2001).

6.5.3 Fecal Excretion and Mass Balance

This comprises compounds secreted across intestinal epithelium, biliary excreted drug and metabolites, and unabsorbed oral drug. Urine, feces, and, if applicable, expired air are collected for mass balance studies until >90% of the radioactive dose is recovered, usually in 7–14 days. Samples are examined for metabolite identification and total radioactivity. Near-full recovery is anticipated; significant loss indicates tissue binding or incomplete collection (Roffey *et al*., 2007).

Clinical decisions are guided by the elimination route. The majority of renal medications need to be adjusted in cases of renal impairment, but they are typically safer in cases of liver disease. When cirrhosis is present, hepatically cleared medications should be used with caution. Adjustments for single-organ dysfunction are rarely necessary for medications with balanced renal and hepatic elimination. For these choices, mass balance studies offer conclusive preliminary data.

6.5.4 Respiratory Excretion

Exhalation can be used to get rid of volatile medications and their metabolites. Oxidative metabolism is measured by measuring $^{13}CO_2$ or $^{13}CO_2$ following the administration of a labeled medication. The degree of oxidation is reflected in the enrichment–time curve: a high recovery of CO_2 (>50 percent) indicates extensive oxidative metabolism, whereas a low recovery indicates incomplete oxidation, conjugation, or renal excretion (Meinert *et al*., 1999).

In vivo, breath tests measure CYP activity. While [^{13}C]caffeine evaluates CYP1A2, the [^{14}C-N-methyl]erythromycin test evaluates CYP3A4 by demethylating it to $^{14}CO_2$. Drug-drug interaction (DDI) risk prediction and dose individualization are supported by these phenotyping tools (Streetman *et al*., 2000).

6.6 Drug-Drug Interaction Studies

CYP induction involves enzyme synthesis over days to weeks, which decreases substrate AUC by 50–90%. Baseline pharmacokinetics are measured, the inducer is administered to steady state (7–14 days), and substrate exposure is reassessed; isotope labeling enhances detection of moderate induction (Madan *et al*., 2003).

Time-dependent inhibition becomes more intense with repeated dosing because of mechanism-based or slow-onset effects. Comparative single-dose versus steady-state studies characterize time-dependent inhibition. For instance, [^{14}C]midazolam studies demonstrated that erythromycin produced more CYP3A4 inhibition after 7 days than after a single dose (Olkkola *et al*., 1993).

6.6 Drug-Drug Interaction Studies

6.6.1 Pharmacokinetic Interactions

Pharmacokinetic Interactions: When one medication modifies the plasma exposure of another, pharmacokinetic DDIs take place. During coadministration, isotope-labeled substrates enable accurate quantification. Substrate pharmacokinetics are compared alone versus with a perpetrator drug; changes in AUC, Cmax, or clearance indicate interaction (Huang *et al*., 2008).

CYP inhibition is prevalent, and strong CYP3A4 inhibitors (e.g., ketoconazole) can cause substrate AUC to increase 5–20 fold. DDI evaluation is required for new drugs with CYP liability, and significant findings may warrant contraindications, dose adjustment, or labeling warnings (U.S. Food and Drug Administration, 2020).

6.6.2 Enzyme Induction and Time-Dependent Interactions

CYP induction involves enzyme synthesis over days to weeks, which decreases substrate AUC by 50–90%. Baseline pharmacokinetics are measured, the inducer is administered to steady state (7–14 days), and substrate exposure is reassessed; isotope labeling enhances detection of moderate induction (Madan *et al*., 2003).

Time-dependent inhibition becomes more intense with repeated dosing because of mechanism-based or slow-onset effects. Comparative single-dose versus steady-state studies characterize time-dependent inhibition. For instance, [^{14}C]midazolam studies demonstrated that erythromycin produced more CYP3A4 inhibition after 7 days than after a single dose (Olkkola *et al*., 1993).

6.6.3 Transporter-Mediated Interactions

Transporter-mediated interactions also affect absorption and disposition, and inhibition, such as P-glycoprotein blockade at the blood–brain barrier, can enhance tissue exposure. Transporter-mediated interactions can be differentiated from CYP-mediated interactions by the use of isotope-labeled substrates (Giacomini *et al*., 2010).

The cocktail approach, which administers several isotope-labeled probes at the same time to evaluate multiple enzymes or transporters in the same study, uses distinct labeling for independent quantification and allows for greater efficiency (e.g., combined probes for CYP3A4, CYP2D6, CYP1A2, and P-glycoprotein can assess multiple pathways in a single clinical trial) (Christensen *et al*., 2003).

6.7 Microdosing Studies

6.7.1 Principles and Applications

Microdosing is a technique that administers sub-therapeutic doses of new drug candidates (≤100 μg or ≤1/100th of the pharmacological dose) labeled with radioisotopes or stable isotopes to determine early human pharmacokinetics (PK); femtomolar–picomolar plasma concentrations can be measured by ultra-sensitive analytical methods. The dose is considered pharmacologically inactive, so first-in-human studies can be carried out with little risk and without extensive toxicology. Because microdosing can be used to assess pharmacokinetics, tissue distribution, target engagement, and drug–drug interactions, the technique is permitted under some regulatory frameworks to be used for evaluating these parameters prior to full clinical development (Lappin & Garner, 2003). Strategically, microdosing avoids compounds with poor absorption, extensive first-pass metabolism, or short half-life before expensive Phase I/II trials, and validates preclinical pharmacokinetic predictions and rational dose selection, which is particularly useful for drugs with safety concerns or oncology agents that cannot be escalated to conventional doses in healthy volunteers (Lappin and Temple, 2006).

6.7.2 Linearity Assessment and Therapeutic Dose Prediction

The assumption of linearity between microdose and therapeutic dose has been confirmed for about 70% of drugs, with discrepancies generally explained by saturable metabolism or transporter-mediated processes (Lappin *et al*., 2005). In a "microdose-plus" design, a labeled microdose is given with or before therapeutic dose, and superimposable, dose-normalized concentration–time curves indicate linearity, whereas deviations suggest nonlinearity.

6.7.3 Microdose Imaging Applications

Microdose imaging with positron emitters (^{11}C, ^{18}F) integrates pharmacokinetics with PET imaging of the distribution and target occupancy for the CNS drug development to directly measure the blood–brain barrier penetration and brain distribution of candidate compounds and to identify early inadequate candidates (Bergström *et al*., 2003). Quantification of receptor occupancy by binding potential allows PET microdosing to guide therapeutic dose selection (often 60–80% occupancy), bridging the preclinical and clinical phases, and providing early human target engagement data with low safety risk.

7.1 ISOTOPE TRACERS IN MOLECULAR BIOLOGY

Molecular biology is the study of the structure and function of DNA, RNA, and proteins, and isotope tracers allow the dynamic measurement of macromolecular synthesis, degradation, modification, and trafficking, unlike static assays, to measure turnover

rates and regulatory mechanisms; from the classic ^{15}N DNA replication study by Meselson & Stahl (1958) that demonstrated that DNA replicates semi-conservatively, to modern stable isotope proteomics that quantifies thousands of proteins simultaneously.

7.2 DNA Replication and Repair Studies

Radioactive thymidine (^{3}H or ^{14}C) and BrdU are incorporated into newly synthesized DNA and S-phase cells can be detected by autoradiography, scintillation counting, or flow cytometry, which showed increased proliferation in tumors and delineated patterns of cell division during embryogenesis. For human studies, non-radioactive alternatives are stable isotopes (^{15}N, ^{13}C-nucleotides) and mass spectrometry. The incorporation of labeled nucleotides at sites of damage can be measured to determine the kinetics of repair synthesis, and to identify active repair pathways.

7.3 RNA Synthesis and Processing

Pulse-labeling with radioactive or stable isotope uridine monitors transcription and RNA maturation, with label appearing first in hnRNA and later in cytoplasmic mRNA, allowing an estimate of processing rates and RNA half-lives; rRNA is very stable (days–weeks), whereas mRNA half-lives vary widely; median mammalian mRNA half-life is ~7–10 hours, while some regulatory transcripts have half-lives of ~30 minutes (Schwanhäusser *et al*., 2011). RNA modifications, such as methylation and pseudouridylation, can be mapped using isotope-labeled methyl donors (e.g., methionine) via mass spectrometry to determine their roles in RNA stability and translational control (Helm & Motorin, 2017).

7.4 Protein Synthesis and Turnover

7.4.1 Measuring Protein Synthesis RatesMeasuring translation rates directly using isotope-labeled amino acids (^{3}H, ^{14}C, ^{13}C). The flooding-dose method (Garlick *et al*., 1980) maximizes precursor amino acid pool enrichment, which is then incorporated into new protein in proportion to the pool enrichment.

The fractional synthesis rate (FSR) of proteins is calculated as:

$$FSR(\%day) = \frac{(\Delta \text{Eprotein})}{(\text{E}precursor \times \text{t})} \times 100$$

where ΔE_protein represents the change in protei-bound amino acid enrichment, E_precursor represents enrichment of the free amino acid pool, and t is labeling time. Protein turnover varies widely: albumin ~20 days; muscle proteins 7–15 days; regulatory proteins hours–days. Humans synthesize and degrade ~250–300 g protein daily (Waterlow, 2006).

7.4.2 Stable Isotope Labeling in Cell Culture (SILAC)

A quantitative proteomics technique called stable isotope labeling by amino acids in cell culture (SILAC) involves growing cells with heavy isotope-labeled amino acids (e.g. The g. [$^{13}C_6{}^{15}N_4$]arginine, [$^{13}C_6{}^{15}C_6$]lysine) until complete incorporation. Mass spectrometry, which resolves 4–10 Da mass shifts to quantify changes in protein abundance, is used to analyze mixed populations that have been differently labeled (light, medium, and heavy) (Ong *et al*. (2002).

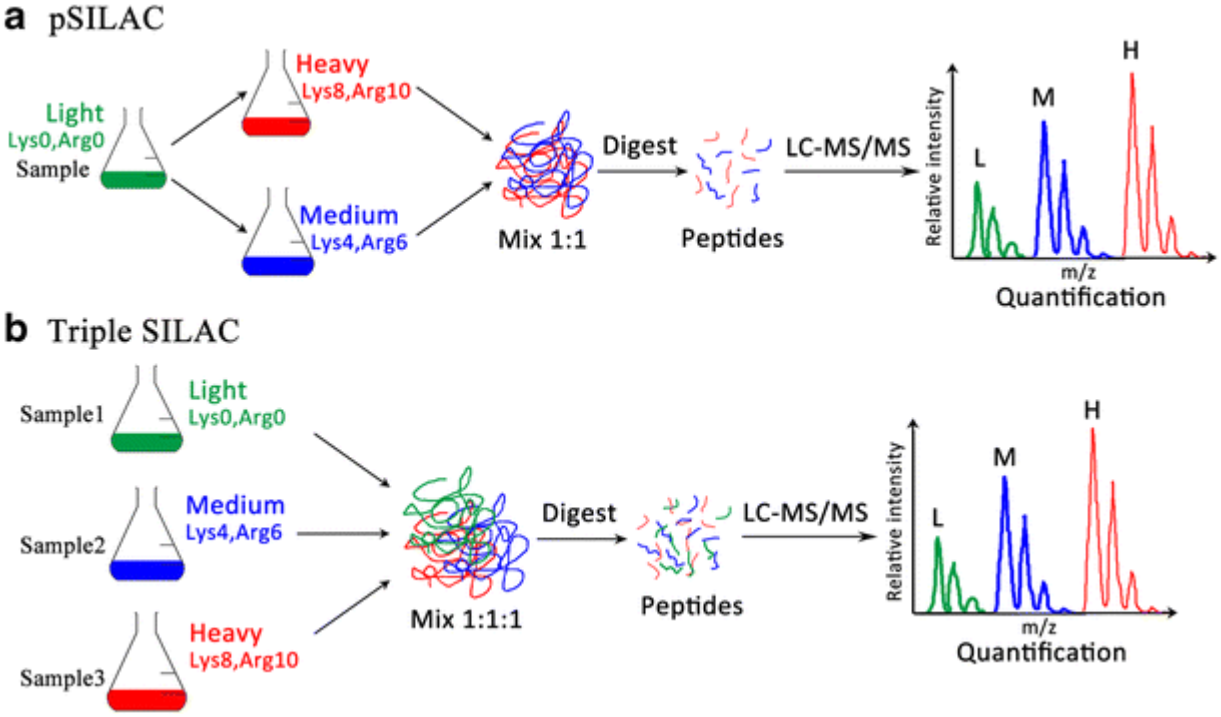

Quantitative Isotope Tracer Methodologies for System-Level Metabolic Flux Analysis and Clinical Translation

The rate of protein turnover has been quantified by alternating cells between heavy and light media and measuring changes in isotope ratio over time using SILAC; rapidly degraded proteins relabel rapidly, whereas stable proteins maintain their original label. Protein half-lives vary from less than 1 hour to greater than 100 hours in mammalian cells, with a median of ~40 to 50 hours, and proteins involved in transcription and signaling turnover most rapidly, whereas structural proteins, histones, and many metabolic enzymes are more stable (Schwanhäusser *et al*., 2011).

7.4.3 In Vivo Protein Turnover

Stable isotope tracers enable measurement of protein turnover in living humans and animals without radiation exposure.

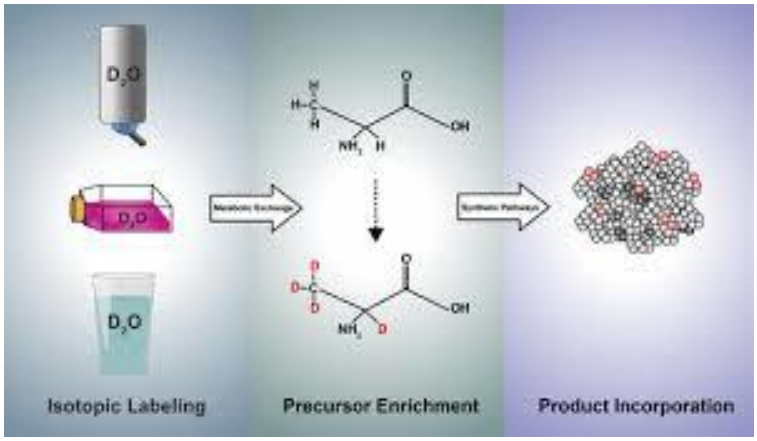

Deuterium oxide (^2H_2O) equilibrates with body water and deuterium is incorporated into amino acids during synthesis; labeled amino acids are then incorporated into newly synthesized proteins. Tissues or body fluids are sampled days to weeks later, proteins are digested, and deuterium incorporation is quantified by peptide mass spectrometry (Busch *et al*., 2006).

8. CLINICAL APPLICATIONS IN MEDICINE

8.1 Oncology and Tumor Metabolism

Cancer cells exhibit metabolic reprogramming, which is characterized by high levels of glycolysis even in the presence of oxygen (Warburg effect). ^{18}F-FDG PET takes advantage of this feature to detect tumors, stage, and monitor treatment; malignant lesions generally have SUV >2.5 and metabolic changes often precede anatomical alterations (Gambhir, 2002).

Tumor metabolism can be further studied using stable isotope tracers, such as [U-$^{13}C_6$]glucose and [U-$^{13}C_5$]glutamine, which are analyzed by LC-MS of surgically obtained tissues and reveal metabolic heterogeneity and glutamine.

Tumor metabolism is further clarified by stable isotope tracers like [U-$^{13}C_6$]glucose and [U-$^{13}C_5$]glutamine. Metabolic heterogeneity and glutamine dependence, including reductive carboxylation of TCA intermediates, are revealed by LC-MS analysis of surgically obtained tissues (Hensley *et al*., 2016), guiding the creation of specific metabolic inhibitors.

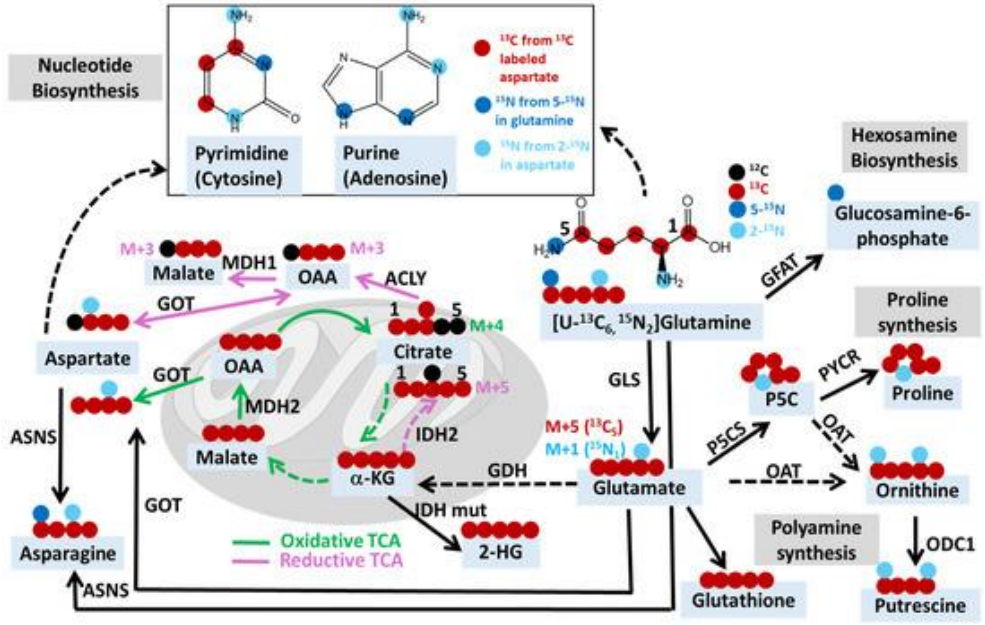

Figure 8.1: Metabolic Fate of [U-$^{13}C_5$, $^{15}N_2$]Glutamine in Tumor Cells

^{13}C and ^{15}N in [U-^{13}C6, 15N2]glutamine may have the following fates, as shown in the schematic above. Abbreviations: MDH (malate dehydrogenase); ACYL (ATP citrate lyase); IDH (isocitrate dehydrogenase); IDH mut (IDH mutant); GDH (glutamate dehydrogenase); GLS (glutaminase); GFAT (fructose-6-phosphate amidotransferase); P5CS (pyrroline-5-carboxylate synthase); PYCR (Δ1-pyrroline-5-carboxylate reductase); OAT (ornithine aminotransferase); ODC1 (ornithine decarboxylase 1); GOT (glutamate-oxaloacetate transaminase 2); ASNS (asparagine synthetase); OAA (oxaloacetate); α-kG (alpha-ketoglutarate); 2-HG (2-hydroxyglutarate); P5C (pyrroline-5-carboxylate).

8.2 Diabetes and Metabolic Disorders

Fasting hyperglycemia in type 2 diabetes is primarily caused by increased HGP, as demonstrated by isotope tracer studies (Consoli *et al*., 1989), which is why the use of metformin, which decreases HGP, is used to treat the condition. The hyperinsulinemic–euglycemic clamp with glucose tracers such as [6,6-$^{2}H_2$]glucose or [U-$^{13}C_6$]glucose is the gold standard for measuring insulin sensitivity (DeFronzo *et al*., 1979), with glucose infusion rate reflecting peripheral insulin sensitivity, and suppression of endogenous glucose production reflecting hepatic sensitivity. This has led to tissue-specific insulin resistance in obesity, PCOS, and lipodystrophy, with hyperinsulinemia (decreased suppression of HGP) as a compensatory response.

8.3 Cardiovascular Disease

Fatty acids (60–70%) and glucose (20–30%) are primarily oxidized by the heart.^{18}F-FDG PET detects hibernating myocardium by identifying preserved glucose uptake despite reduced perfusion, and aids in revascularization decisions (Schelbert *et al*., 2003). Evaluation of fatty acid metabolism employs ^{11}C-palmitate PET or [U-$^{13}C_{16}$]palmitate infusion with arteriovenous sampling and has demonstrated impaired fatty acid oxidation in heart failure, which contributes to energetic and contractile dysfunction.

8.4 Neurology and Brain Metabolism

8.4 Neurology and Brain Metabolism The brain accounts for only 2% of body mass, but consumes ~20% of total energy. ^{18}F-FDG PET reveals disease-specific hypometabolic patterns: temporoparietal and posterior cingulate regions in Alzheimer's disease; frontal/anterior temporal regions in frontotemporal dementia; and focal interictal hypometabolism in epilepsy (Herholz, 2010). ^{18}F-DOPA PET measures dopamine synthesis and is used for early diagnosis and monitoring of Parkinson's disease.

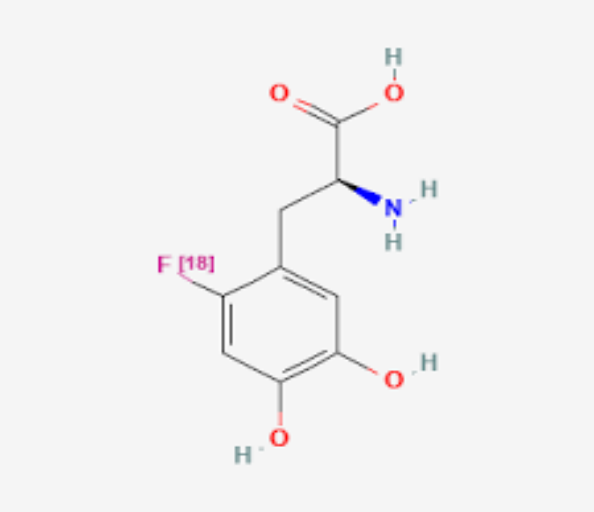

6-[^{18}F]fluoro-L-3,4-dihydroxyphenylalanine

Figure 8.2: ^{18}F-DOPA PET Imaging of Dopaminergic Function

Structure and metabolic pathway of 6-[^{18}F]fluoro-L-3,4-dihydroxyphenylalanine (^{18}F-DOPA). After transport across the blood–brain barrier, ^{18}F-DOPA is decarboxylated to fluorodopamine and stored in synaptic vesicles. Reduced striatal ^{18}F-DOPA uptake indicates dopaminergic degeneration and can detect subclinical disease in at-risk individuals (Brooks, 2010).

8.5 Protein and Lipid Metabolism

The most definitive method of quantifying human protein turnover is the use of isotope tracers, where stable isotope-labeled amino acids (^{13}C- or ^{15}N-leucine) are most commonly used; fasting plasma leucine appearance reflects whole-body proteolysis, while $^{13}CO_2$ enrichment in breath quantifies leucine oxidation, and protein synthesis is calculated as appearance minus oxidation and intake (Wolfe & Chinkes, 2005).

Protein synthesis in muscle is measured using the precursor–product method, which measures the incorporation of a tracer into muscle following infusion and biopsy, and demonstrates that resistance exercise increases synthesis for 24–48 h, that distributed protein intake increases the anabolic response, and that aging results in anabolic resistance that is overcome with higher doses of protein (Burd *et al*., 2013).

Stable isotopes are used to measure VLDL production, cholesterol kinetics, and de novo lipogenesis (DNL) in lipid metabolism. After administration of $^{2}H_2O$, deuterium incorporation into fatty acids measures the contribution of DNL, which increases to ~30% of liver triglyceride in non-alcoholic fatty liver disease, compared to <5% in healthy individuals (Donnelly *et al*., 2005).

9. INSTRUMENTATION FOR ISOTOPE DETECTION

9.1 Mass Spectrometry Systems

Instrumentation for Isotope Detection9.1 Mass Spectrometry SystemsGC-C-IRMS oxidizes GC-separated compounds to CO_2 and measures $^{13}C/^{12}C$ ratios with 0.1–0.5‰ precision at nanomole levels (Barrie & Prosser 1996).

Triple quadrupole instruments perform selected reaction monitoring (SRM), achieving femtomole–attomole sensitivity for tracer quantification in complex matrices (Chace, 2001).

Orbitrap analyzers determine ion oscillation frequency to deliver ultra-high resolution (up to 1,000,000) and <1 ppm accuracy, resolving fine isotopic structure and low-abundance isotopologues (Zubarev & Makarov 2013).

9.2 Nuclear Imaging Systems

Using LSO/LYSO crystals, PET has 4–6 mm resolution; time-of-flight improves localization (Cherry *et al*., 2012).

Hybrid PET/CT and PET/MRI combine metabolic and anatomical imaging, and MRI provides better soft tissue contrast without ionizing radiation (Pichler *et al*., 2010).

SPECT uses rotating gamma cameras with lead collimators; it is less sensitive (0.01–0.1% vs 1–5%) but accommodates longer-lived isotopes at lower cost, with 7–15 mm resolution (Khalil *et al*., 2011).

9.3 Liquid Scintillation Counting

Liquid scintillation counters employ coincidence photomultiplier detection and pulse height analysis to differentiate beta emitters; they rely on quench correction to achieve counting efficiencies of ~60–65% for ^{14}C and 40–50% for ^{3}H in biological samples (L'Annunziata, 2012).

10. DATA ANALYSIS AND QUANTIFICATION

10.1 Isotope Ratio Calculations

Quantification of stable isotope enrichment requires calculating isotope ratios from mass spectrometric data and correcting for natural abundance contributions. When analyzing ^{13}C enrichment, measured ion abundances must be corrected for the approximately 1.1% natural abundance of ^{13}C. Atom percent excess (APE) expresses enrichment as the percentage of labeled atoms above natural abundance:

$$APE = \left(\frac{R_{sample} - Rnatural}{1 + Rsample}\right) \times 100$$

where R represents the isotope ratio (heavy/light isotope abundance). Sophisticated algorithms perform these corrections for complex molecules containing multiple elements (Wolfe & Chinkes, 2005).

10.2 Metabolic Flux Analysis

Metabolic flux analysis (MFA) uses isotope labeling data to quantify intracellular reaction rates. ^{13}C-MFA combines experimental mass isotopomer distributions with computational models of metabolism to calculate fluxes that best explain observed labeling patterns. The steady-state metabolic system is described by mass balance equations, with isotope labeling providing additional constraints through isotopomer balance equations. Non-linear optimization algorithms solve for flux distributions that minimize differences between simulated and measured isotopologue distributions (Antoniewicz, 2015).

10.3 Kinetic Modeling

Compartmental modeling describes tracer kinetics using differential equations representing mass balance in physiological compartments. For PET imaging, kinetic modeling converts tissue time-activity curves into physiological parameters. The Patlak plot provides a graphical method for irreversible tracer uptake, such as ^{18}F-FDG phosphorylation, yielding the influx constant K_i that quantifies metabolic rate. More detailed analyses use full kinetic models with rate constants for transport, phosphorylation, and dephosphorylation estimated by curve fitting (Phelps *et al*., 1979).

SAFETY AND REGULATORY CONSIDERATIONS

- **Radiation Safety**

Use of radioactive tracers requires adherence to the ALARA (As Low as Reasonably Achievable) principle. Effective dose accounts for absorbed dose and biological effectiveness of different radiation types. Typical diagnostic nuclear medicine procedures produce effective doses of 1-20 mSv, comparable to 0.5-10 years of natural background radiation (approximately 2-3 mSv/year). For ^{18}F-FDG PET, administered activity of 370-740 MBq produces an effective dose of approximately 5-10 mSv (Mettler *et al*., 2008).

Regulatory limits in the United States specify 50 mSv per year for occupational exposure, 5 mSv per year for the general public, and 0.5 mSv for pregnancy in declared pregnant workers. Time, distance, and shielding principles minimize personnel exposure during radioisotope handling.

- **Ethical and Regulatory Framework**

Research involving isotope tracers requires institutional review board approval, informed consent, and often radiation safety committee review. Vulnerable populations including children and pregnant women require special protections. Stable isotopes offer safe alternatives for studying metabolism in these populations. Data management follows Good Clinical Practice guidelines, including protocol adherence, accurate record-keeping, and protection of participant confidentiality (International Conference on Harmonisation, 1996).

CONCLUSION

In clinical medicine and biomedical research, isotope tracers have become indispensable tools to precisely and quantitatively explore biological processes, because the isotope behaves chemically like the natural element but has a distinct, measurable physical property. As a result of advances in analytical technologies, metabolic research is now a highly quantitative science rather than a descriptive science. Radioisotopes (e.g.) provide high sensitivity and real-time imaging, whereas stable isotopes (H, C, N, and O) are safe for use in vulnerable populations. These tools have been used to clarify glycolysis, TCA cycle dynamics, gluconeogenesis, cancer cell metabolism, and many other pathways. Isotope tracers also have been a significant contributor to clinically relevant advancements in oncology (^{18}F-FDG PET imaging, for example).

REFERENCES

1) American Diabetes Association. (2014). Diagnosis and classification of diabetes mellitus. *Diabetes Care*, *37*(Supplement 1), S81–S90. https://doi.org/10.2337/dc14-S081
2) American Diabetes Association. (2023). Classification and diagnosis of diabetes: Standards of care in diabetes—2023. *Diabetes Care*, *46*(Supplement_1), S19–S40. https://doi.org/10.2337/dc23-S002
3) American Society for Hybrid, Molecular and Translational Imaging (2024). *ESR essentials: Staging and restaging with FDG-PET/CT in oncology—Practice recommendations by the European Society for Hybrid, Molecular and Translational Imaging. European Radiology*. https://link.springer.com/article/10.1007/s00330-024-11094-8 (PubMed)
4) Antoniewicz, M. R. (2015). Methods and advances in metabolic flux analysis: A mini-review. *Journal of Industrial Microbiology & Biotechnology*, *42*(3), 317-325. https://doi.org/10.1007/s10295-015-1585-x
5) Ayeni, A., Evbuomwan, O., & Vangu, M.-D. T. W. (2025). The role of ^{18}F-FDG PET/CT in monitoring of therapy response in lung cancer. *Seminars in Nuclear Medicine*, *55*(2), 175–189. https://doi.org/10.1053/j.semnuclmed.2025.02.002
6) Barrie, A., & Prosser, S. J. (1996). Automated analysis of light-element stable isotopes by isotope ratio mass spectrometry. In T. W. Boutton & S. Yamasaki (Eds.), *Mass spectrometry of soils* (pp. 1-46). Marcel Dekker.
7) Basu, R., Chandramouli, V., Dicke, B., Landau, B., & Rizza, R. (2006). Obesity and type 2 diabetes impair insulin-induced suppression of glycogenolysis as well as gluconeogenesis. *Diabetes, 54*(7), 1942-1948. https://doi.org/10.2337/diabetes.54.7.1942
8) Bier, D. M. (1987). The use of stable isotopes in metabolic investigation. *Baillière's Clinical Endocrinology and Metabolism, 1*(4), 817-836. https://doi.org/10.1016/s0950-351x(87)80007-1

9) Bier, D. M. (1997). Stable isotopes in metabolic research: Applications and perspectives. *The Journal of Clinical Investigation*, *99*(6), 1133–1137. https://doi.org/10.1172/JCI119270
10) Brooks, D. J. (2010). Imaging approaches to Parkinson disease. *Journal of Nuclear Medicine, 51*(4), 596-609. https://doi.org/10.2967/jnumed.108.059998
11) Burd, N. A., West, D. W., Moore, D. R., Atherton, P. J., Staples, A. W., Prior, T., Tang, J. E., Rennie, M. J., Baker, S. K., & Phillips, S. M. (2013). Enhanced amino acid sensitivity of myofibrillar protein synthesis persists for up to 24 h after resistance exercise in young men. *Journal of Nutrition*, *143*(4), 876-880. https://doi.org/10.3945/jn.110.135038
12) Busch, R., Kim, Y. K., Neese, R. A., Schade-Serin, V., Collins, M., Awada, M., Gardner, J. L., Beysen, C., Marino, M. E., Misell, L. M., & Hellerstein, M. K. (2006). Measurement of protein turnover rates by heavy water labeling of nonessential amino acids. *Biochimica et Biophysica Acta*, *1760*(5), 730-744. https://doi.org/10.1016/j.bbagen.2005.12.023
13) Calderoni, L., Giovanella, L., & Fanti, S. (2024). Endocrinology application of molecular imaging: Current role of PET/CT. *Journal of Endocrinological Investigation*, *47*(10), 2383–2396. https://doi.org/10.1007/s40618-024-02400-8
14) Chace, D. H. (2001). Mass spectrometry in the clinical laboratory. *Chemical Reviews, 101*(2), 445-478. https://doi.org/10.1021/cr990077+
15) Cherry, S. R., Sorenson, J. A., & Phelps, M. E. (2012). *Physics in nuclear medicine* (4th ed.). Elsevier Saunders.
16) Cherry, S. R., Sorenson, J. A., & Phelps, M. E. (2021). *Physics in nuclear medicine* (5th ed.). Elsevier.
17) Calderoni, L., Giovanella, L., & Fanti, S. (2024). Endocrinology applications of molecular imaging: Current role of PET/CT. *Journal of Endocrinological Investigation*, *47*(10), 2383–2396. https://doi.org/10.1007/s40618-024-02400-8
18) Cobelli, C., Toffolo, G., Bier, D. M., & Nosadini, R. (1987). Models to interpret kinetic data in stable isotope tracer studies. *American Journal of Physiology-Endocrinology and Metabolism, 253*(5), E551-E564. https://doi.org/10.1152/ajpendo.1987.253.5.E551
19) Consoli, A., Nurjhan, N., Capani, F., & Gerich, J. (1989). Predominant role of gluconeogenesis in increased hepatic glucose production in NIDDM. *Diabetes*, *38*(5), 550-557. https://doi.org/10.2337/diab.38.5.550
20) DeFronzo, R. A., Tobin, J. D., & Andres, R. (1979). Glucose clamp technique: A method for quantifying insulin secretion and resistance. *American Journal of Physiology-Endocrinology and Metabolism, 237*(3), E214-E223. https://doi.org/10.1152/ajpendo.1979.237.3.E214
21) Des Rosiers, C., Fernandez, C. A., David, F., & Brunengraber, H. (1994). Reversibility of the mitochondrial isocitrate dehydrogenase reaction in the perfused rat liver: Evidence from isotopomer analysis of citric acid cycle intermediates. *Journal of Biological Chemistry, 269*(44), 27179-27182. https://doi.org/10.1016/S0021-9258(18)46979-9
22) Dimitrakopoulou-Strauss, A., Pan, L., & Sachpekidis, C. (2024). Non-[^{18}F]FDG PET-radiopharmaceuticals in oncology. *Pharmaceuticals*, *17*(12), 1641. https://doi.org/10.3390/ph17121641
23) Donnelly, K. L., Smith, C. I., Schwarzenberg, S. J., Jessurun, J., Boldt, M. D., & Parks, E. J. (2005). Sources of fatty acids stored in liver and secreted via lipoproteins in patients with nonalcoholic fatty liver disease. *Journal of Clinical Investigation*, *115*(5), 1343-1351. https://doi.org/10.1172/JCI23621
24) European Society for Hybrid, Molecular and Translational Imaging. (2024). ESR essentials: Staging and restaging with FDG-PET/CT in oncology-Practice recommendations. *European Radiology, 34*(11), 7432-7445. https://doi.org/10.1007/s00330-024-11094-8
25) Gambhir, S. S. (2002). Molecular imaging of cancer with positron emission tomography. *Nature Reviews Cancer*, *2*(9), 683-693. https://doi.org/10.1038/nrc882
26) Giacomini, K. M., Huang, S. M., Tweedie, D. J., Benet, L. Z., Brouwer, K. L., Chu, X., Dahlin, A., Evers, R., Fischer, V., Hillgren, K. M., Hoffmaster, K. A., Ishikawa, T., Keppler, D., Kim, R. B., Lee, C. A., Niemi, M., Polli, J. W., Sugiyama, Y., Swaan, P. W., ... Zhang, L. (2010). Membrane transporters in drug development. *Nature Reviews Drug Discovery*, *9*(3), 215-236. https://doi.org/10.1038/nrd3028
27) Goodman, K. J., & Brenna, J. T. (1992). High sensitivity tracer detection using high-precision gas chromatography-combustion isotope ratio mass spectrometry and highly enriched [U-^{13}C]-labeled precursors. *Analytical Chemistry*, *64*(11), 1088-1095. https://doi.org/10.1021/ac00034a004
28) Hall, K. D. (2012). Energy balance and its components: Implications for body weight regulation. *The American Journal of Clinical Nutrition*, *95*(4), 989–994. https://doi.org/10.3945/ajcn.112.036350
29) Hall, K. D., & Guo, J. (2017). Obesity energetics: Body weight regulation and the effects of diet composition. *Gastroenterology*, *152*(7), 1718–1727.e3. https://doi.org/10.1053/j.gastro.2017.01.052
30) Hellerstein, M. K. (1999). Measurement of lipid synthesis and turnover in humans using stable isotopes. *Journal of Lipid Research*, *40*(3), 433–456. https://doi.org/10.1016/S0022-2275(20)32139-4
31) Helm, M., & Motorin, Y. (2017). Detecting RNA modifications in the epitranscriptome: Predict and validate. *Nature Reviews Genetics*, *18*(5), 275-291. https://doi.org/10.1038/nrg.2016.169

32) Hensley, C. T., Faubert, B., Yuan, Q., Lev-Cohain, N., Jin, E., Kim, J., Jiang, L., Ko, B., Skelton, R., Loudat, L., Wodzak, M., Klimko, C., McMillan, E., Butt, Y., Ni, M., Oliver, D., Torrealba, J., Malloy, C. R., Kernstine, K., ... DeBerardinis, R. J. (2016). Metabolic heterogeneity in human lung tumors. *Cell, 164*(4), 681-694. https://doi.org/10.1016/j.cell.2015.12.034

33) Herholz, K. (2010). Cerebral glucose metabolism in preclinical and prodromal Alzheimer's disease. *Expert Review of Neurotherapeutics, 10*(11), 1667-1673. https://doi.org/10.1586/ern.10.136

34) Hop, C. E., Wang, Z., Chen, Q., & Kwei, G. (1998). Plasma-pooling methods to increase throughput for in vivo pharmacokinetic screening. *Journal of Pharmaceutical Sciences, 87*(7), 901-903. https://doi.org/10.1021/js970486q

35) Huang, S. C. (2000). Anatomy of SUV. *Nuclear Medicine and Biology, 27*(7), 643-646. https://doi.org/10.1016/S0969-8051(00)00155-4

36) Huang, S. M., Strong, J. M., Zhang, L., Reynolds, K. S., Nallani, S., Temple, R., Abraham, S., Al-Habet, S. A., Baweja, R. K., Burckart, G. J., Chung, S., Colangelo, P., Frucht, D., Green, M. D., Hepp, P., Karnaukhova, E., Ko, H. S., Lee, J. I., Marroum, P. J., ... Throckmorton, D. C. (2008). New era in drug interaction evaluation: US Food and Drug Administration update on CYP enzymes, transporters, and the guidance process. *Journal of Clinical Pharmacology, 48*(6), 662-670. https://doi.org/10.1177/0091270007312153

37) International Atomic Energy Agency. (2021). *Radiation safety of radionuclide sources and tracers: Fundamentals and standards*. Vienna Austria: IAEA.

38) International Atomic Energy Agency. (2022). *Doubly labelled water method for measuring energy expenditure: Human health series*. IAEA.

39) International Conference on Harmonisation. (1996). *ICH harmonised tripartite guideline: Guideline for good clinical practice E6(R1)*. https://database.ich.org/sites/default/files/E6_R1_Guideline.pdf

40) Isin, E. M., Elmore, C. S., Nilsson, G. N., Thompson, R. A., & Weidolf, L. (2012). Use of radiolabeled compounds in drug metabolism and pharmacokinetic studies. *Chemical Research in Toxicology, 25*(3), 532-542. https://doi.org/10.1021/tx2005212

41) Jang C, Chen, L., & Rabinowitz, J. D. (2022). Metabolomics and isotope tracing. *Cell, 185*(2), 247–267. https://doi.org/10.1016/j.cell.2021.12.010

42) Kelleher, J. K., & Masterson, T. M. (1992). Model equations for condensation biosynthesis using stable isotopes and radioisotopes. *American Journal of Physiology-Endocrinology and Metabolism, 262*(1), E118-E125. https://doi.org/10.1152/ajpendo.1992.262.1.E118

43) Khalil, M. M., Tremoleda, J. L., Bayomy, T. B., & Gsell, W. (2011). Molecular SPECT imaging: An overview. *International Journal of Molecular Imaging, 2011*, Article 796025. https://doi.org/10.1155/2011/796025

44) Khojasteh, S. C., Oishi, S., & Nelson, S. D. (2011). Metabolism and toxicity of menthofuran in rat liver slices and in rats. *Chemical Research in Toxicology, 24*(12), 2123-2133. https://doi.org/10.1021/tx200291b

45) Kim, S. Y., Chung, H. W., So, Y., Lee, M. H., & Lee, E. J. (2024). Recent updates of PET in lymphoma: FDG and beyond. *Biomedicines, 12*(11), 2485. https://doi.org/10.3390/biomedicines12112485

46) Klein, S., & Wolfe, R. R. (2022). Stable isotopes in clinical metabolic research: Applications in human physiology and disease. *The American Journal of Clinical Nutrition, 115*(6), 1505–1516. https://doi.org/10.1093/ajcn/nqac044

47) Knoll, G. F. (2010). *Radiation detection and measurement* (4th ed.). John Wiley & Sons.

48) Landau, B. R., Wahren, J., Chandramouli, V., Schumann, W. C., Ekberg, K., & Kalhan, S. C. (1996). Contributions of gluconeogenesis to glucose production in the fasted state. *Journal of Clinical Investigation, 98*(2), 378-385. https://doi.org/10.1172/JCI118803

49) L'Annunziata, M. F. (2012). *Handbook of radioactivity analysis* (3rd ed.). Academic Press.

50) Lappin, G., & Temple, R. (2006). *Radiotracers in drug development*. CRC Press.

51) Lappin, G., Kuhnz, W., Jochemsen, R., Kneer, J., Chaudhary, A., Oosterhuis, B., Drijfhout, W. J., Rowland, M., & Garner, R. C. (2005). Use of microdosing to predict pharmacokinetics at the therapeutic dose: Experience with 5 drugs. *Clinical Pharmacology and Therapeutics, 77*(3), 203-215. https://doi.org/10.1016/j.clpt.2004.11.001

52) Madan, A., Graham, R. A., Carroll, K. M., Mudra, D. R., Burton, L. A., Krueger, L. A., Downey, A. D., Czerwinski, M., Forster, J., Ribadeneira, M. D., Gan, L. S., LeCluyse, E. L., & Parkinson, A. (2003). Effects of prototypical microsomal enzyme inducers on cytochrome P450 expression in cultured human hepatocytes. Drug Metabolism and Disposition, 31(4), 421–431. https://doi.org/10.1124/dmd.31.4.421

53) Magnusson, I., Rothman, D. L., Katz, L. D., Shulman, R. G., & Shulman, G. I. (1992). Increased rate of gluconeogenesis in type II diabetes mellitus: A ^{13}C nuclear magnetic resonance study. *Journal of Clinical Investigation, 90*(4), 1323-1327. https://doi.org/10.1172/JCI115997

54) Meselson, M., & Stahl, F. W. (1958). The replication of DNA in Escherichia coli. *Proceedings of the National Academy of Sciences, 44*(7), 671-682. https://doi.org/10.1073/pnas.44.7.671

55) Mettler, F. A., Huda, W., Yoshizumi, T. T., & Mahesh, M. (2008). Effective doses in radiology and diagnostic nuclear medicine: A catalog. *Radiology, 248*(1), 254-263. https://doi.org/10.1148/radiol.2481071451
56) Nelson, D. L., & Cox, M. M. (2017). Lehninger principles of biochemistry (7th ed.). New York, NY: W. H. Freeman. https://www.macmillanlearning.com/college/us/product/Lehninger-Principles-of-Biochemistry/p/1319108245
57) Nobel Prize Outreach. (2023). George de Hevesy—Biographical. https://www.nobelprize.org/prizes/chemistry/1943/hevesy/biographical/
58) Obach, R. S. (1999). Prediction of human clearance of drugs from in vitro data. Drug Metabolism and Disposition, 27(11), 1350–1359. https://dmd.aspetjournals.org/content/27/11/1350
59) Ogilvie, B. W., Zhang, D., Li, W., Rodrigues, A. D., Gipson, A. E., Holsapple, J., Toren, P., & Parkinson, A. (2008). Glucuronidation converts xenobiotics to toxic products. Chemical Research in Toxicology, 21(4), 760–767. https://doi.org/10.1021/tx7004059
60) Olkkola, K. T., Ahonen, J., & Neuvonen, P. J. (1993). The effects of enzyme inhibitors on drug metabolism. Clinical Pharmacokinetics, 24(2), 105–121. https://doi.org/10.2165/00003088-199324020-00002
61) Ong, S. E., Blagoev, B., Kratchmarova, I., Kristensen, D. B., Steen, H., Pandey, A., & Mann, M. (2002). Stable isotope labeling by amino acids in cell culture, SILAC, as a simple and accurate approach to expression proteomics. *Molecular & Cellular Proteomics, 1*(5), 376-386. https://doi.org/10.1074/mcp.M200025-MCP200
62) Patterson, B. W., Carraro, F., & Wolfe, R. R. (1993). Measurement of ^{15}N enrichment in multiple amino acids and urea in a single analysis by gas chromatography/mass spectrometry. *Biological Mass Spectrometry, 22*(9), 518-523. https://doi.org/10.1002/bms.1200220908
63) Patterson, B. W., Zhao, G., Elias, N., Hachey, D. L., & Klein, S. (2002). Validation of a new procedure to determine plasma fatty acid concentration and isotopic enrichment. *Journal of Lipid Research, 43*(5), 720–727. https://doi.org/10.1016/S0022-2275(20)30467-X
64) Penner, N., Klunk, L. J., & Prakash, C. (2009). Human radiolabeled mass balance studies: Objectives, utilities and limitations. Biopharmaceutics & Drug Disposition, 30(4), 185–203. https://doi.org/10.1002/bdd.659
65) Phelps, M. E. (2000). Positron emission tomography provides molecular imaging of biological processes. *Proceedings of the National Academy of Sciences, 97*(16), 9226-9233. https://doi.org/10.1073/pnas.97.16.9226
66) Phelps, M. E., Huang, S. C., Hoffman, E. J., Selin, C., Sokoloff, L., & Kuhl, D. E. (1979). Tomographic measurement of local cerebral glucose metabolic rate in humans with (F-18)2-fluoro-2-deoxy-D-glucose: Validation of method. *Annals of Neurology, 6*(5), 371-388. https://doi.org/10.1002/ana.410060502
67) Pichler, B. J., Kolb, A., Nägele, T., & Schlemmer, H. P. (2010). PET/MRI: Paving the way for the next generation of clinical multimodality imaging applications. *Journal of Nuclear Medicine, 51*(3), 333-336. https://doi.org/10.2967/jnumed.109.061853
68) Piel, M., Vernaleken, I., & Rösch, F. (2014). Positron emission tomography in CNS drug discovery and drug monitoring. *Journal of Medicinal Chemistry, 57*(22), 9232-9258. https://doi.org/10.1021/jm5001858
69) Roberts, M. S., Magnusson, B. M., Burczynski, F. J., & Weiss, M. (2002). Enterohepatic circulation: Physiological, pharmacokinetic and clinical implications. *Clinical Pharmacokinetics, 41*(10), 751-790. https://doi.org/10.2165/00003088-200241100-00005
70) Roffey, S. J., Obach, R. S., Gedge, J. I., & Smith, D. A. (2007). What is the objective of mass balance studies in humans? Drug Metabolism Reviews, 39(1), 17–43. https://doi.org/10.1080/03602530601032238
71) Rowland, M., & Tozer, T. N. (2011). *Clinical pharmacokinetics and pharmacodynamics: Concepts and applications* (4th ed.). Philadelphia, PA: Lippincott Williams & Wilkins.
72) Schelbert, H. R., Beanlands, R., Bengel, F., Knuuti, J., Di Carli, M., Machac, J., & Patterson, R. (2003). PET myocardial perfusion and glucose metabolism imaging: Part 2—Guidelines for interpretation and reporting. *Journal of Nuclear Cardiology, 10*(5), 557-571. https://doi.org/10.1016/S1071-3581(03)00666-3
73) Schwanhäusser, B., Busse, D., Li, N., Dittmar, G., Schuchhardt, J., Wolf, J., Chen, W., & Selbach, M. (2011). Global quantification of mammalian gene expression control. *Nature, 473*(7347), 337-342. https://doi.org/10.1038/nature10098
74) Schwochau, K. (1994). Technetium radiopharmaceuticals—Fundamentals, synthesis, structure, and development. *Angewandte Chemie International Edition in English, 33*(22), 2258-2267. https://doi.org/10.1002/anie.199422581
75) Shipkova, M., & Wieland, E. (2001). Glucuronidation in therapeutic drug monitoring. Clinical Chimica Acta, 313(1–2), 43–57. https://doi.org/10.1016/S0009-8981(01)00605-8
76) Solon, E. G., Kraus, A., & Schmitz, R. (2010). Methods for assessing tissue distribution of drugs. Current Drug Metabolism, 11(9), 798–809. https://doi.org/10.2174/138920010793175895
77) Steele, R. (1959). Influences of glucose loading and of injected insulin on hepatic glucose output. *Annals of the New York Academy of Sciences, 82*(2), 420-430. https://doi.org/10.1111/j.1749-6632.1959.tb44923.x

78) Streetman, D. S., Bertino, J. S., Jr., & Nafziger, A. N. (2000). Phenotyping of drug-metabolizing enzymes in humans. Clinical Pharmacokinetics, 38(5), 347–365. https://doi.org/10.2165/00003088-200038050-00002
79) Timmins, P. (2014). The utility of mass balance studies in drug development. Drug Metabolism and Disposition, 42(1), 3–7. https://doi.org/10.1124/dmd.113.053231
80) U.S. Food and Drug Administration. (2003). Guidance for industry: Bioavailability and bioequivalence studies. Rockville, MD: Author. Retrieved from https://www.fda.gov/regulatory-information/search-fda-guidance-documents
81) Wolfe, R. R. (1992). *Radioactive and stable isotope tracers in biomedicine: Principles and practice of kinetic analysis*. Wiley-Liss.
82) Wolfe, R. R., & Chinkes, D. L. (2005). *Isotope tracers in metabolic research: Principles and practice of kinetic analysis* (2nd ed.). John Wiley & Sons.
83) Wolfe, R. R., & Chinkes, D. L. (2017). *Isotope tracers in metabolic research: Principles and practice of kinetic analysis* (2nd ed.). Wiley.
84) Wolfe, R. R., Chinkes, D. L., & Ferrando, A. A. (2020). Isotope tracers in metabolic research: Applications in nutrition and human disease. *Clinical Nutrition*, *39*(3), 631–646. https://doi.org/10.1016/j.clnu.2019.09.020
85) Zanger, U. M., & Schwab, M. (2013). Cytochrome P450 enzymes in drug metabolism: Regulation of gene expression, enzyme activities, and impact of genetic variation. Pharmacology & Therapeutics, 138(1), 103–141. https://doi.org/10.1016/j.pharmthera.2012.12.007